Interactions of a covalently - linked antithrombin-heparin complex with components of the fibrinolytic pathway

Ankush Chander, M.B., B.S

A Thesis

Submitted to the School of Graduate Studies

in Partial Fulfillment of the Requirements

for the Degree

Master of Science

McMaster University

MASTER OF SCIENCE (2013) McMaster University

(Medical Sciences) Hamilton, ON

TITLE: The interactions of a covalently-linked antithrombin-heparin complex with components of the fibrinolytic pathway

AUTHOR: Dr. Ankush Chander

SUPERVISOR: Dr. Anthony Chan

NUMBER OF PAGES: LXXXVI

Abstract

Unfractionated heparin (UFH) is used as an adjunct during thrombolytic therapy. However, its use is associated with many clinical limitations, such as the inability to inhibit fibrin-bound coagulation factors, increasing the potential for sustained procoagulant activity. We have developed a covalent conjugate of antithrombin (AT) and heparin (ATH) with superior anticoagulant properties to those of UFH. Some advantages of ATH include enhanced inhibition of surface-bound enzymes and its ability to reduce the overall size and mass of clots *in vivo*. However, the potential interactions of UFH or ATH with the components of the fibrinolytic pathway are not well understood. Therefore, our study utilized discontinuous second order rate constant (k_2) assays to determine rates of inhibition of plasmin (Pn) in the presence or absence of fibrin by AT+UFH *vs.* ATH. In addition, we monitored the rates of Pn generation in a system comprised of preformed fibrin clots with the aim of evaluating the inhibitory effect of AT+UFH or ATH in this more native system. The k_2 values for the inhibition of Pn without fibrin were $5.74x10^6 \pm 0.278x10^6$ and $6.39x10^6 \pm 0.588x10^6$ for AT+UFH and ATH, respectively (p=0.36). In the presence of fibrin, the k_2 values decreased to $1.45x10^6 \pm 0.0971x10^6$ for AT+UFH and $3.07x10^6 \pm 0.192x10^6$ for ATH ($p<0.05$). Therefore, protection of Pn by fibrin is observed for both inhibitors. Pn generation also decreased in the presence of both inhibitors, with the greatest reduction (approx. 38-fold) observed for ATH, even at the lowest concentration tested. Although both inhibitors were capable of inhibiting Pn, the inhibition rates were 2 to 3 orders of magnitude lower than those achieved for inhibition of other coagulation factors, such as thrombin. Cumulatively, these data may indicate that, relative to coagulant enzymes, components of the fibrinolytic system may be spared

from inhibition by both AT+UFH and ATH, thus limiting reduction in fibrinolytic potential during anticoagulant therapy.

Acknowledgments

I would like to thank Dr. Anthony Chan for providing me with this valuable opportunity to work as a part of his research team. I would also like to express my appreciation to Helen Atkinson and Leslie Berry for their continuing guidance and support over the course of my project. Additionally I am thankful to Drs. Mark Hatton and Gonzalo Hortelano and Leslie Berry for agreeing to be on my committee and mentoring me as I progressed through this project. I would also like to thank Dr. Ivan Stevic who has been an invaluable resource to me throughout this project.

Table of Contents

List of figures

List of Tables

List of Abbreviations

aPTT	Activated partial thromboplastin time
AT	Antithrombin
ATH	Covalent antithrombin-heparin complex
AT+UFH	Non-covalent antithrombin-unfractionated heparin complex
Fn	Fibrin
Fg	Fibrinogen
FII	Factor II or prothrombin
FV	Factor V
FVII	Factor VII
FVIII	Factor VIII
FIX	Factor IX
FX	Factor X
FXI	Factor XI
FXII	Factor XII
XIII	Factor XIII
FIIa	Activated factor II or thrombin
FVIIa	Activated factor VII

FIXa	Activated factor XI
FXa	Activated factor X
FXIa	Activated factor XI
FXIIa	Activated factor XII
FXIIIa	Activated factor XIII
GAG	Glycosaminoglycan
k_1	pseudo first-order rate constant
k_2	second-order rate constant
LMWH	Low molecular weight heparin
PAGE	Polyacrylamide gel electrophoresis
PAR-1	Protease activated receptor 1
PAR-2	Protease activated receptor 2
Pg	Plasminogen
Pn	Plasmin
RCL	Reactive center loop
SDS PAGE	Sodium dodecyl sulphate polyacrylamide gel electrophoresis
TBS-T80	Tris(hydroxymethyl) aminomethane saline buffer with Tween-80
TAFI	Thrombin activatable fibrinolysis inhibitor

TF	Tissue Factor
TFPI	Tissue factor pathway inhibitor
TM	Thrombomodulin
tPA	Tissue plasminogen activator
TSP	Tris (hydroxymethyl) aminomethane saline buffer with polyethylene glycol
V_o	Initial enzyme activity
V_t	Enzyme activity at time t
UFH	Unfractionated heparin
uPA	Urokinase- plasminogen activator

1. Introduction

1.1 Overview

Under physiological conditions, blood is maintained in the fluid state allowing the delivery of nutrients and removal of waste from tissues. A fine balance exists between the coagulation and fibrinolytic cascades such that fibrin generation and breakdown is maintained in a steady state. (1) Thrombosis ensues when this balance tips in favour of FIIa generation and subsequent fibrin polymerization. Clinically under such situations, anticoagulants such as unfractionated heparin (UFH) are used to limit the generation of FIIa and subsequent clot formation. (2) As well as interacting with the components of the coagulation pathway, UFH also has the potential to interact with the fibrinolytic pathway. (3-13) Our laboratory has developed a novel covalently-linked antithrombin-heparin (ATH) complex which has been shown to be a superior inhibitor of coagulation enzymes when compared to non-covalent mixtures of antithrombin (AT) and UFH. (14) Furthermore, in vivo studies have demonstrated the ability of ATH to prevent clot formation and reduce clot mass in thrombosis models. (15,16) However, the mechanisms involved in this reduction of clot mass are unknown and the interactions of ATH with components of the fibrinolytic pathway have not been studied before. Thus, in an effort to gain a better understanding, the current study examines the possible interactions of ATH with components of the fibrinolytic pathway.

1.2 Thrombosis

The hemostatic mechanism which prevents blood loss from the vasculature can be life threatening when the delicate balance between procoagulant and anticoagulant components favour FIIa formation. Thrombi can develop in either the venous or the arterial circulation producing various degrees of vessel occlusion, potentially leading to significant morbidity and mortality. Central to these conditions is either increased clot formation or decreased degradation of a formed clot (Figure 1). (17,18) The life threatening nature of these events often requires urgent interventions to re-establish the vital flow of blood to the oxygen and nutrient deprived tissues. Under such circumstances anticoagulants such as UFH are administered in an attempt to restore hemostasis. Many of the existing anticoagulants are associated with adverse risks such as excessive and sometimes life threatening bleeding which limit their utility as therapeutic agents.

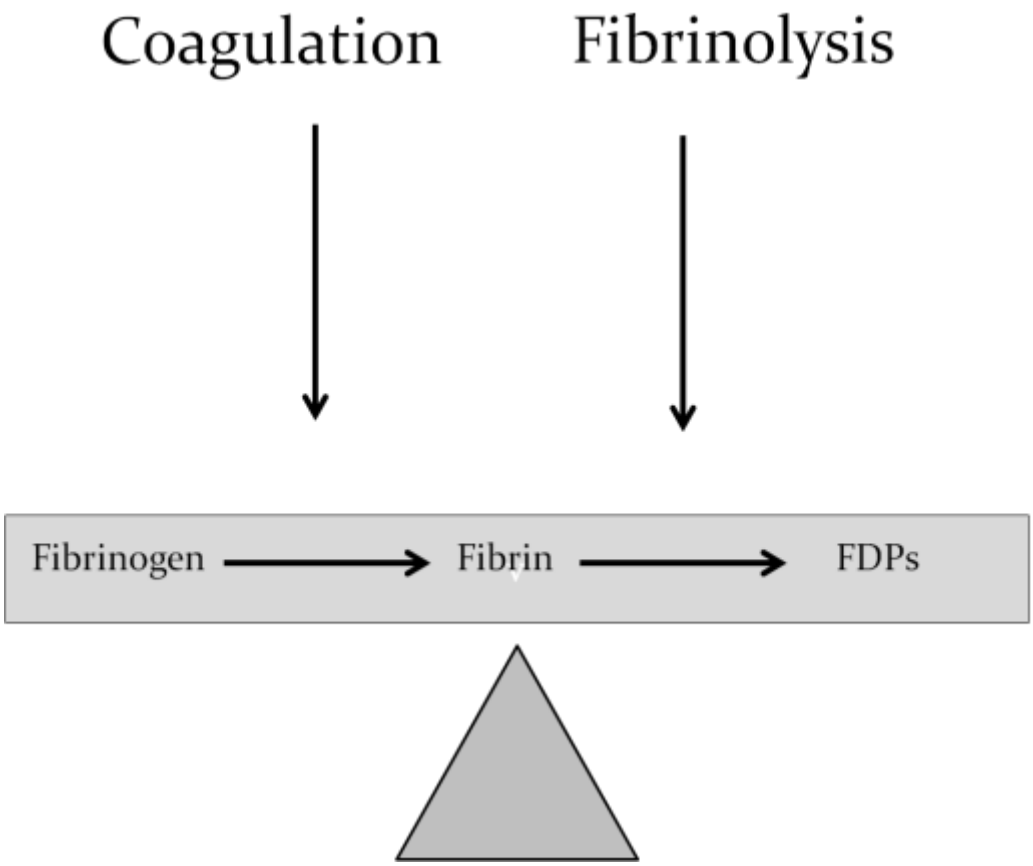

Figure 1. The balance between coagulation and fibrinolysis

Hemostasis is a balance between the coagulation and the fibrinolytic pathways.

An imbalance in these two processes can result in thromboembolism. (1)

1.3 Coagulation

Coagulation plays a pivotal role in hemostasis and serves to arrest blood loss at sites of vessel injury, thus maintaining the integrity of the cardiovascular system. (19) Coagulation is a complex biochemical process which involves the interaction of a series of serine proteases and receptor/cofactor counterparts on membrane surfaces. (20) These coagulation factors generally circulate in inactive states (zymogens) until they are activated through proteolysis by an upstream factor. (21) The waterfall cascade model has been used to depict the interactions occurring in coagulation leading to the formation of FIIa and subsequent fibrin polymerization. (22,23) In this model two distinct pathways are described, the extrinsic and the intrinsic pathways, which ultimately lead to the formation of the prothrombinase complex and subsequent FIIa generation (figure 2). (22) Recently, a cell based model has also been proposed in an effort to address how coagulation occurs *in vivo*. This was developed after it was observed that the deficiency of factor FXII did not lead to bleeding disorders in the presence of a prolonged activated partial thromboplastin time (aPTT). (24) The cell based model stresses the roles that cells may play in the control of the duration, intensity and location of coagulation in an overlapping manner. (24) Coagulation ultimately leads to the formation of FIIa which cleaves fibrinogen to form fibrin monomer resulting in the self-assembly of a fibrin clot. (20)

Using the cell based model, coagulation can be divided into three phases, initiation, amplification and propagation. Coagulation is initiated by the exposure of extra-vascular tissue factor (TF) to the blood which can occur during vessel injury or plaque rupture. (25) During the initiation phase, TF complexes with FVIIa which then is

able to activate small amounts of factor FIX and factor FX. (25) At this point factor FXa complexes with FVa to form the prothrombinase complex in the presence of calcium and phospholipids, which then cleaves small amounts of FII to FIIa. (24) In the next stage termed the amplification phase, the FIIa formed during the initiation phase cleaves and activates, FV, FVIII and FXI resulting in further FIIa formation. (24) During this phase, FIIa also acts as a potent stimulator of platelets which have migrated to the sites of injury, resulting in the release of the contents of their granules. Additionally, platelets also provide a phospholipid surface for the formation of coagulation complexes. (24) Subsequently, FIXa and FVIIIa then come together on negatively-charged phospholipid surfaces, to form the tenase complex in the presence of calcium and FXa complexes with FVa to form the prothrombinase complex on cell surfaces. (24) These events then lead to a rapid burst of FIIa generation during the final propagation phase leading to the formation of fibrin monomers and fibrin polymerization, resulting in the formation of a stable platelet - rich fibrin clot. (24) (figure 2)

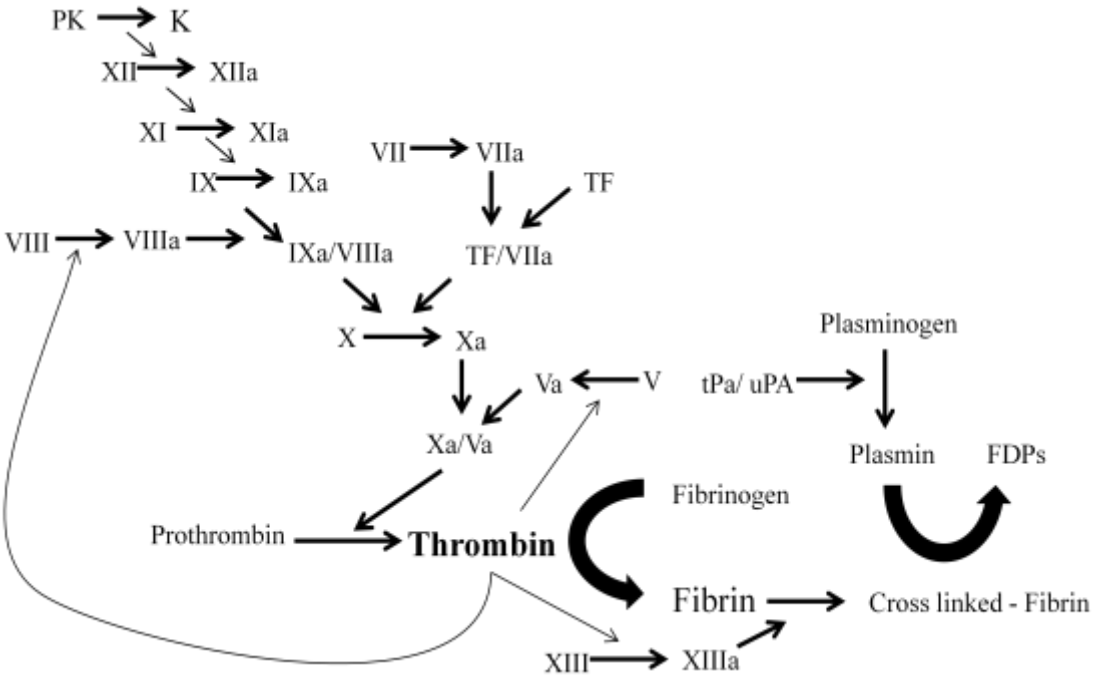

Figure 2. The coagulation cascade

Coagulation factors are depicted by roman numerals with activated forms followed by the letter a. tPA: tissue type plasminogen activator; uPA: urokinase type plasminogen activator; FDPs: Fibrin degradation products, TF: tissue factor, PK: Prekallikrein, K; Kallikrein (24)

1.4 Fibrinolysis

During the formation of a fibrin-clot, the fibrinolytic pathway is activated. (figure 3). Physiologically the fibrinolytic pathway serves to restrict excessive clot formation beyond the site of vessel injury. Plasmin (Pn) is the key proteolytic enzyme of the fibrinolytic pathway. The zymogen, plasminogen (Pg) is secreted as a single-chain 90 kDa protein primarily by the liver and once cleaved into Pn consists of a heavy chain and a light chain. Located on the heavy chain of plasmin are five kringle (K) domains. (26-28) The catalytic triad is located in the light chain and consists of His^{603}, Asp^{646}, and Ser^{741}. (29) Pg activators, (tissue type Pg activator (tPa) or urokinase type Pg activator (uPa)) cleave the circulating zymogen, Pg, at its Arg^{560}-Val^{561} bond, forming the serine protease Pn (figure 4). (30) Pn can enhance its own generation by cleavage of single chain tPA (sc- tPA) at its Arg^{275} - Ile^{276} peptide bond, to form a more active disulphide-linked two-chain polypeptide, two chain tPA (tc-tPA). (31) There are two forms of Pg found *in vivo*, Glu - Pg which has a glutamate residue at its amino terminus and Lys-Pg which has a lysine at its amino terminus. (32) It is thought that Glu - Pg is first converted into Lys-Pg, and then finally into Pn, and that Glu - Pg is the form found primarily in the circulation, whereas Lys- Pg is primarily found bound to fibrin. (32,33) Lys - Pg is able to bind fibrin more avidly and is activated 10-20 times more rapidly than Glu - Pg. (30,34)

Fibrin acts both as a substrate and as a co-factor for the activation of Pg. (28) When bound to fibrin, tPA cleaves Pg rapidly, resulting in the formation of Pn and the breakdown of the fibrin meshwork and subsequent fibrin depletion which limits plasmin formation. (35) In the absence of fibrin the affinity between tPA and Pg is relatively low.

(35) It has been suggested that fibrin binds both tPA and Pg simultaneously, which results in a conformational change in the structure of tPA making it more reactive towards Pg, thus enhancing plasmin generation. (35-37) Once fibrin is cleaved by Pn, C-terminal Lysine (C-Lys) residues are exposed on the surfaces of the fibrin clots. Both tPA and Pg contain Lys binding domains (LBDs) which allow for the localization of tPa and Pg in close proximity. (28,37) The binding of Pg to fibrin occurs through Kringle (K) domains located on the Pg molecule. (26) This interaction takes place with all K domains except K3, with K1 and K4 exhibiting the strongest affinities for lysine type ligands. (27,38) Similarly, uPA can also cleave Pg to Pn and is an effective Pg activator both in the presence and absence of fibrin. (39,40) Thus, tPa mediated Pn generation and fibrinolysis remain localized to the site of thrombus formation. After the cross linking of adjacent fibrin monomeric units by factor XIIIa, the proteolytic action of Pn on various peptide bonds in the fibrin clot leads to the formation of products known as fibrin degradation products (FDPs) . (41)

The binding of Pg to fibrin can be inhibited both by the administration of therapeutic agents and by naturally occurring regulators. Activated thrombin activatable fibrinolysis inhibitor (TAFIa) removes C-Lys residues from fibrin clots, thus preventing binding of PG and tPA and subsequently the formation of the tri-molecular fibrin-Pg-tPA complex and ultimately Pn generation. (42) Binding to C-Lys can also be inhibited by the therapeutic administration of epsilon-aminocaproic acid (EACA) or tranexamic acid (which are structural analogues of Lys), thus inhibiting the binding of Pg and tPA with fibrin. (43,44)

Pn is primarily regulated by a plasma serine protease inhibitor (serpin) alpha 2-antiplasmin (α_2-AP), which is produced by the liver and which is also a constituent of platelet α - granules. (45,46) The action of α_2-AP is consistent with the general mechanisms of serpins: after cleavage of Arg^{364} - Met^{365} of the reactive center loop of α_2-AP by Pn, an irreversible α_2-AP-Pn complex is formed, followed by a rapid clearance of this complex by the liver. (47) It is accepted that inhibition of Pn by α_2-AP occurs in a two-step mechanism in which unavailability of the LBDs reduces the rate of inhibition. (48-50) These studies suggest that α_2-AP first interacts weakly with the LBDs on plasmin followed by interaction with the active site of the protease. Investigators have demonstrated that the rate of inhibition of Pn by α_2-AP is reduced when inhibition is performed with low molecular weight forms of Pn which lack the K domains. (49)

It is well known that coagulation enzymes are protected from inhibition when bound to surfaces such as fibrin and phospholipid membranes. (51,52) Similarly, Pn when bound to fibrin is protected from inhibition by its natural inhibitor α_2-AP. (53,54) Pn is also inhibited to a lesser extent by the protein, α_2-macroglobulin which is synthesized by endothelial cells and macrophages, and which is also found in platelet α - granules. (55) Although not a serpin, α_2 - macroglobulin can form non-covalent complexes with Pn, thereby inhibiting its activity. (56) In a similar fashion, the Pg activators are regulated predominately by the serpin Pg activator inhibitor-1 (PAI-1) which is secreted by endothelium, leukocytes, hepatocytes, adipocytes and by platelets. (57,58) PAI-1 acts rapidly to inhibit both tPA and uPA and is the most important inhibitor of the Pg activators. (59) PAI-1 is secreted in the initial stages of fibrin clot

formation and serves to inhibit early clot dissolution. PAI-2 is also an inhibitor of Pg activators but significant levels are found in plasma only during pregnancy. (60)

Clinically, the process of fibrinolysis can be induced by the intravenous administration of therapeutic levels of tPA in the acute stages of a thromboembolic event. The tPA administered therapeutically acts in the same manner described above. Early administration of thrombolytic agents has been shown to reduce mortality and thus is widely used in these situations. During this stage, adjuvant therapy such as anti-platelet drugs and anticoagulants such as UFH are also used to counteract the process of vessel re-occlusion, a major problem associated with the use of thrombolytics. (61)

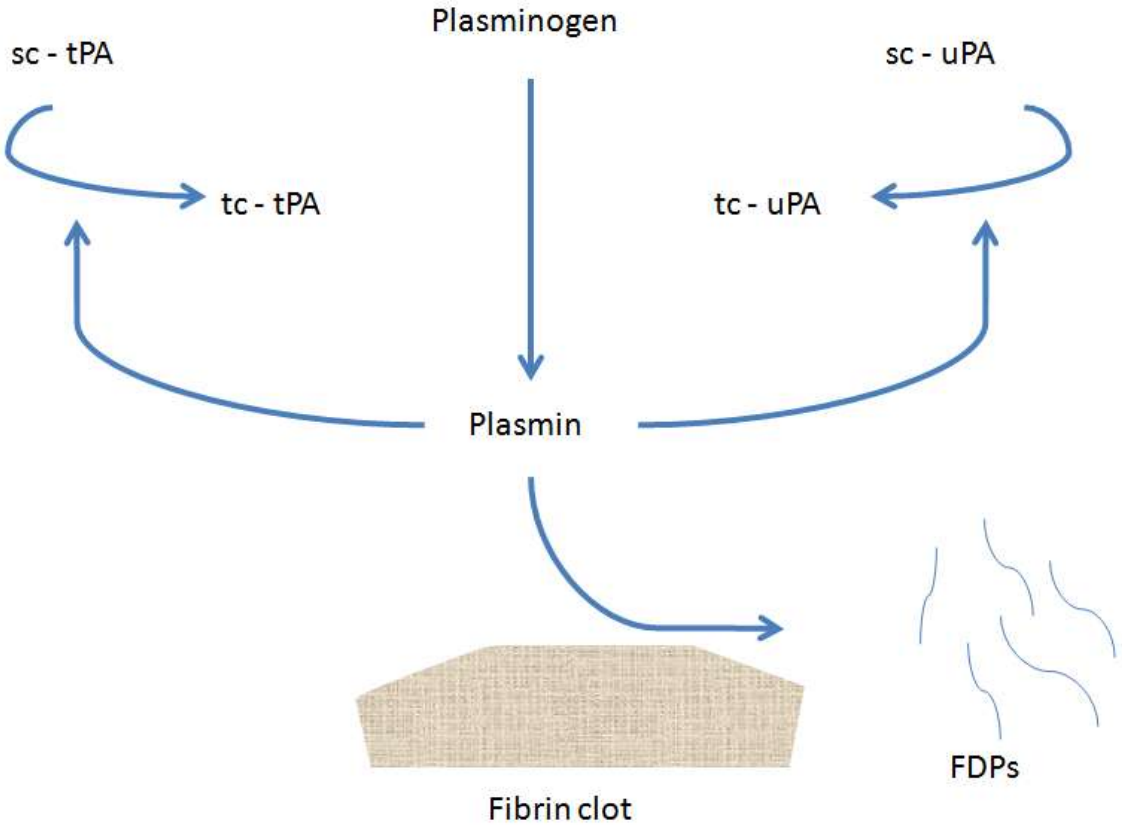

Figure 3. The fibrinolytic pathway

Pn is formed by cleavage of the zymogen Pg by a Pg activator. Pn can cleave sc – tPA and sc-uPA into active tc-tPA and active tc-uPa, respectively. Sc - tPA: Single chain tissue Pg activator, sc-uPA: single chain urokinase Pg activator, tc - tPA - two chain tissue Pg activator, tc – uPA: two chain urokinase Pg activator, PAI: Pg activator inhibitor, α_2-AP: α_2 anti-plasmin, α_2- MG: α_2-macroglobulin. (55)

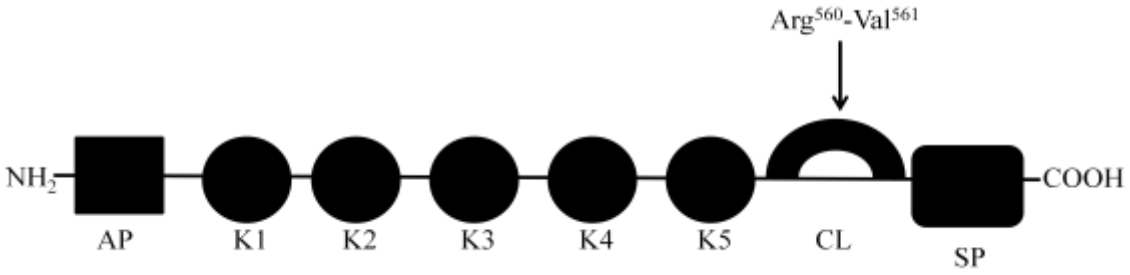

Figure 4. The Pg molecule

Five kringle domains follow the 77 residue activation peptide (AP). Following the five K domains is the cleavage loop (CL) which is cleaved by Pg activators at the Arg^{560} – Val^{561} peptide bond leading to Pn formation. The serine protease domain (SP) overlaps with the CL. (62)

1.5 Antithrombin

Coagulation is highly regulated by a number of biological inhibitors including serpins. (24) AT, a glycoprotein, is a member of the serpin super family and the key inhibitor of coagulation. (63) Structurally, AT consists of three β-sheets, nine α-helices and a reactive centre loop (RCL) which protrudes above its surface. (64) It is synthesized by the hepatocytes and has a plasma concentration of 150µg/ml and a half life of approximately 3 days. (64) AT inhibits FVIIa, FIXa, FXa, FXIIa and FIIa irreversibly by forming 1:1 enzyme - inhibitor complexes, but is primarily active against FIIa and FXa. (65-69) The RCL houses a specific peptide bond which is referred to as P1-P1' and gives AT selectivity towards various serine proteases. (70) During cleavage of the P1-P1' peptide bond by the target serine protease, an ester bond is formed between the α-carbonyl on the P1 residue of the serpin and the hydroxyl group of the serine residue of the enzyme. (70,71) Subsequently, the cleaved RCL which is still covalently linked to the protease, inserts into the major beta sheet thus translocating the protease from the top to the bottom of the serpin molecule inactivating the enzyme. (71-73)

Two isoforms of AT exist in the circulation, with 90% in the alpha isoform and the remaining 10% in the beta isoform. Although the two isoforms possess the highly conserved structure of the serpin family, the two differ in their degree of glycosylation. Human alpha antithrombin consists of complex type N-linked glycans on asparagine residues 96, 135, 155 and 192 and the beta form possesses only three N-glycans, lacking the glycan at position 135. (64,74)

1.6 Heparin

A member of the glycosaminoglycan (GAG) family, heparin is a linear polysaccharide which consists of repeating uronic acid - glucosamine disaccharide units. (75,76) *In vivo*, heparin is synthesized and stored in mast cells and is released at sites of inflammation. (77,78) UFH has been used therapeutically for its anticoagulant properties in the treatment and prevention of thromboembolism for the past 80 years. Structurally, heparin is a highly heterogeneous polymer due to the variability of its molecular weight (MW) and its monosaccharide components. Commercial UFH consists of a wide MW range of constituent molecules (3-25 kDa) The glucosamine residues can either be N-acetylated or N-sulphated and the uronic acid present can occur as either D-glucuronic acid or L-iduronic acid. (75,76) Additionally, heparin has a highly negative charge due to the variable N- and O-sulfation of the disaccharide units. (79)

The anticoagulant effect imparted by heparin is due to its ability to catalyze the inhibition of clotting factors by binding AT. (80) In the absence of UFH, the inhibition of clotting factors by AT occurs at a relatively slow rate while in its presence this inhibition can be accelerated up to one thousand fold. (3) The presence of characteristic pentasaccharide sequences on heparin chains allow AT molecules to bind to the polysaccharide, this in turn results in a conformational change in AT which favours its reaction towards clotting factors. (3,75,81) AT binds to a specific pentasaccharide sequence on heparin, via its heparin binding domain located on the D helix, which leads to structural changes. (82,83) The structural changes in the AT lead to the increased exposure of the inserted portion of the RCL which attracts certain procoagulant serine proteases such as FIIa to cleave the exposed reactive amino acid residues. (78,80)

1.6.1 Mechanism of inhibition catalysis by heparin

Heparin has been shown to mediate the inhibition of clotting enzymes by AT *via* two distinct mechanisms. These mechanisms can be reflected by determination of the relationship between second order rate constants (k_2) for enzyme inhibition versus UFH concentrations. These methods yield characteristic plots which can suggest the mechanism of inhibition (figure 5). (3,14)

In the conformational AT activation mechanism the UFH chain binds to the AT molecule resulting in a conformation of AT which is more reactive towards the target serine protease, as is the case with FXa inhibition. In the heparin catalyzed inhibition of FXa by AT, an initial increase in the k_2 values is seen, followed by a plateau of rates with increasing concentrations of UFH. (3,84)

In the template mediated inactivation mechanism, the UFH chain binds both AT and the target serine protease such as FIIa, which results in a conformational change in AT, as well as brings the inhibitor and protease in close proximity. (84-86) For the formation of this complex a minimum heparin chain length of at least 18 disaccharides is necessary, which explains why low molecular weight heparins (LMWH) <18 saccharides in length have a decreased ability to accelerate the AT mediated inhibition of FIIa. (85) In this mechanism a characteristic bell shaped curve can be observed in which k_2 values increases to a maximum and then decline as the concentration of UFH is further increased. (3,14) This decline in observed rates is a result of the formation of non-covalent complexes between the enzyme and UFH chains, in addition to the AT-UFH complexes. (3) As a result of this formation, the AT-UFH complex is unable to access the enzyme bound to the heparin chain. (3)

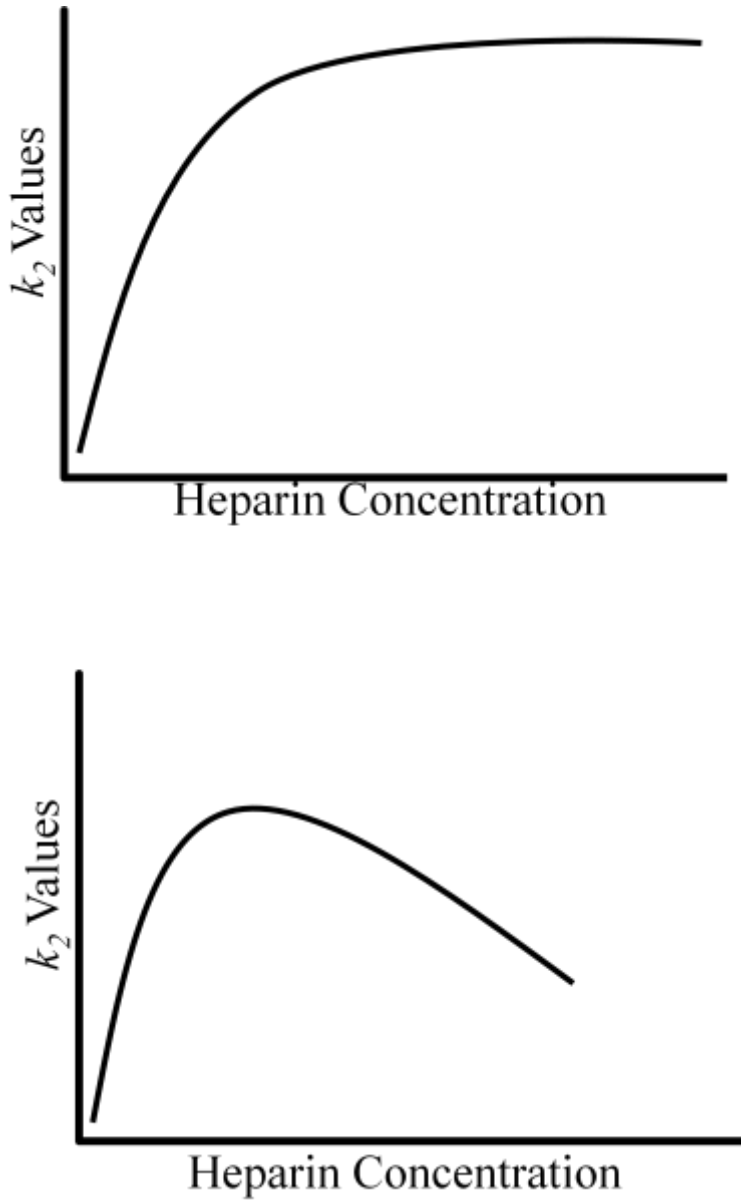

Figure 5. Illustrations of characteristic plots for conformational AT activation and template-mediated inactivation. A) Conformational AT activation and B) Template-mediated inactivation

Adapted from, Patel S., 2005. Inhibition of Coagulation Cascade Enzymes by a Covalent Antithrombin-Heparin (Masters of Science Thesis) McMaster University

1.6.2 Limitations of Heparin

Although UFH is widely used in clinical practice for the treatment and prophylaxis of thromboembolic diseases, there are a number of drawbacks associated with its use. UFH binds non-specifically to plasma proteins and cell surfaces reducing the ability of AT to bind to heparin, limiting its catalytic activity. (87) The relatively small molecular size of heparin allows it to pass through tissue layers and thus is unable to sequester in vascular spaces. (88) The above two pharmacokinetic properties of UFH result in an unpredictable anticoagulant response and large individual variation. (89) For these reasons patients who are receiving heparin must be continuously monitored to ensure that the desired level of anticoagulation is being achieved. The major biophysical limitation of UFH is its inability to inhibit surface bound coagulation factors such as fibrin-bound FIIa, and phospholipid-bound factor FXa. (51,90,91) Clinical evidence indicates that fibrin-bound FIIa activity is an important source for thrombus extension and the primary mediator of the early re-occurrence of acute coronary syndromes seen soon after discontinuation of UFH therapy. (92) Fibrin and heparin can bind to FIIa through interaction with exosite-1 and exosite-2 respectively, leaving fibrin bound FIIa relatively protected from inhibition by non-covalent AT+UFH. (51,91) Finally, only one third of commercially available preparations of UFH contain the high affinity pentasaccharide sequence and thus two thirds of the heparin preparations are unable to catalyze the inhibition of clotting factors. (93)

1.7 Heparin and the fibrinolytic pathway

There is a potential for heparin to interact with various components of the fibrinolytic pathway. Various studies have made an effort to elucidate the interactions of heparin with the fibrinolytic pathway; however the results of these studies have been conflicting.

Pn, a serine protease, is susceptible to inhibition by AT. (3,4,94) Studies have shown that in the presence of heparin this inhibition is accelerated 20-100 fold. (3,4,94) k_2 values for the inhibition of Pn by AT have been reported to be 10^4-10^5 M^{-1} min^{-1} in the absence of heparin and 10^6 M^{-1} min^{-1} with heparin present. (3,4) However it has been demonstrated, by both *in vivo* and *in vitro* experiments, that this inhibition results in the neutralization of only approximately 2-4% of Pn at therapeutic levels of heparin and may play a limited role *in vivo*. (5-7)

There is much debate regarding heparin's interactions with tPA. Many *in vitro* studies have demonstrated that heparin can inhibit (95), enhance (9,95-100) or have no effect (95,99,101) on tPA mediated generation of Pn. Markwardt *et al* found that when a pig ear was perfused with heparin, an increase in tPA levels was seen in a dose dependent manner. (8) *In vitro* experiments reported by Andrade-Gordon and Strickland suggested that heparin may enhance tPA mediated Pn generation. (100) In this study, Andrade-Gordon *et al* reported an increase in tPA mediated Pn generation by heparin in a dose dependent manner. (100) Similar results were demonstrated in kinetic studies which showed that the presence of heparin led to a 5.3 fold increase in the catalytic rate of tPA and a subsequent increase in Pn generation. (96)

It has also been suggested that heparin and fibrin compete for the same binding site on the tPA molecule. However, fibrin and heparin do not exhibit an additive effect on the generation of Pn except at low concentrations of fibrin. (9,98) This is thought to occur because fibrin binds tPA more than 10-fold stronger than does heparin. (98,100) Similarly, several other *in vitro* studies have suggested that heparin can enhance the rate of Pg activation by tPA. (10,11,98) It has been shown that LMWH does not affect plasmin generation, and only heparin chains of high molecular weight (> 17 kDa) can enhance tPA-mediated Pn generation. (11,12) Recent studies have reported enhanced tPA activity on the presence of UFH while demonstrating no modification of activity by the direct effects of heparin on Pn. (98)

Several studies have suggested that the interaction of heparin and tPA is sensitive to salt concentrations in the absence of fibrinogen and, that in physiological ionic strength, heparin fails to stimulate tPA mediated plasmin generation. (99)

1.8 Covalently-linked ATH Complex

Due to the complex biochemical and biophysical properties of UFH, treatments are often complicated by the unpredictable level of anticoagulation. Thus, the need for an alternative therapeutic agent with superior anticoagulant properties has led to the development of a covalently-linked antithrombin-heparin complex (ATH). The synthesis of a covalently-linked ATH complex has been attempted by various groups, each yielding a product with varying degrees of anticoagulant activity and viability. (102-104)

1.8.1 Synthesis of ATH complex

Chan *et al* have developed a method of ATH synthesis which yields high percentage of active product possessing a superior anticoagulant properties when compared to non-covalent mixtures of AT+UFH. (14,16,105-107) This synthetic method utilizes the principles of non-enzymatic glycation a process commonly occurring in the plasma of diabetic individuals. (105) It is observed in the plasma of diabetic individuals, that some plasma proteins undergo non-enzymatic covalent conjugation with plasma glucose by a Schiff base/Amadori rearrangement mechanism, the products of which can survive in the body for years. (108) After the formation of a Schiff base (imine) between the aldehyde functional group on C_1 plasma glucose and the ε – amino group on the lysyl residues of proteins, a metastable product is formed that is in equilibrium with its starting components. (108) This metastable molecule can then be driven to form a keto-amine through a tautomeric Amadori rearrangement under appropriate conditions involving glucose concentrations, pH, temperature and amino group availability. (108) Similarly, the synthesis of ATH involves the linkage of a plasma protein (AT) to an aldose containing polysaccharide unit (UFH), thus allowing the principles of Schiff Base/Amadori rearrangement to be applied to yield a covalently linked product. (105)

It has been shown previously that the glycation of AT is a selective event which occurs approximately once per AT molecule. (109) It has also been shown that if AT is reacted under appropriate conditions with excess amounts of aldose-terminating heparin a covalent linkage could be established without modification of the AT or UFH. (109) With this knowledge, Chan *et al* applied these principles for synthesis of an ATH complex as follows. AT and a molar excess of UFH (>200 - fold) are reacted for up to 14 days in a

physiological buffer at 40^{o}C, followed by removal of unconjugated AT and heparin by chromatographic methods. (105) Excess UFH is removed using butyl-Sepharose hydrophobic chromatography and excess AT is removed using DEAE Sepharose anion exchange chromatography. (105) The resultant product is a covalently bound AT and UFH complex in which a spontaneous Schiff Base formation and an Amadori rearrangement have occurred. (105) Investigations have determined that the covalent linkage occurs between the terminal aldose on the UFH chain and the N - terminal amino acid His1 or the Ɛ- amino group of Lys139 with relative proportions of 87% and 13% respectively. (110)

1.8.2 Properties of ATH

ATH has been shown to be a superior anticoagulant compared to non-covalent AT+UFH for a number of reasons. The rate limiting step in the catalysis of inhibition of FIIa by AT is the binding and subsequent activation of AT by UFH. (107) Due to the covalent linkage between AT and UFH, AT is permanently in its active state at the time of administration, which allows for rapid inactivation of coagulation factors. (14,107)

Several experiments have been done to demonstrate the superiority of ATH over AT+UFH. Methods used to produce the covalent conjugate have yielded 50% ATH using the novel glycation method. (111) ATH has been shown to contain 55% α-AT, and 45% β-AT, a higher proportion of the more reactive β-AT than found in plasma. (112,113) Rate experiments have demonstrated that the k_2 values for ATH inhibition of FIIa is 2.6 x 10^9 $M^{-1}min^{-1}$ which is four-fold faster than the maximal rate measured for AT+UFH (7.3 x 10^8 $M^{-1}min^{-1}$). (107) Additionally, it has been shown that ATH is able to inhibit fibrin bound FIIa and prothrombinase bound FXa significantly faster than non-covalent

AT-UFH. (106,114-116) It has also been determined that ATH is able to not only directly inhibit coagulation factors but was also able to catalyze inhibition of FIIa or FXa by exogenous AT. (107) This is in part attributable to the fact that a significant proportion of the heparin chains in ATH possess more than one pentasaccharide sequence allowing for ATH to bind up to 1.5 exogenous molecules of AT. (107) Furthermore, in vivo studies utilizing rabbit thrombosis models have also been done. Thrombosis prevention models demonstrated that ATH administration prevented thrombus formation after the induction of endothelial injury compared to the development of thrombosis with comparable doses of UFH and control groups. (15) Similarly, rabbit thrombosis treatment models showed a reduction in clot mass with the administration of ATH (17%) compared to an increase in clot mass with the administration of UFH, UFH+AT or saline (60%, 24%, 135% respectively). (16) These findings suggest that ATH may potentially directly or indirectly augment the fibrinolytic pathway resulting in improved vessel patency with ATH. It has been demonstrated *in vivo* that ATH has a longer half-life when compared to UFH, with a major reason being ATH's reduced degree of binding to non-specific plasma and endothelial surface proteins, as well as its larger molecular weight. (105,117) *In vivo* studies have shown that ATH possesses an α-phase intravenous half-life of 2.6 hr compared to 0.32 hr of a similar dose of UFH; this is equivalent to an eight - fold extension of half-life of UFH. (105) ATH possesses heparin chains of larger length averaging 18 kDa, which is in part the reason behind ATH's ability to inhibit coagulation factors faster using a template mediated mechanism. (105)

1.9 Overall Aim

The overall aim of the current study was to examine potential interactions of AT+UFH *versus* ATH with components of the fibrinolytic system.

1.10 Hypotheses

In comparison to AT+UFH, ATH will interact with components of the fibrinolytic pathway differently. Since Pn has been reported to be inhibited by a conformational AT activation, rates for the inhibition of the free enzyme by ATH will be similar to those achieved by AT+UFH. Interactions of Pn+fibrin(ogen) will be significantly different than free Pn with ATH showing greater rates of inhibition. ATH will reduce Pn generation to a greater extent than AT+UFH by effective inhibition of fibrin-bound Pn.

1.11 Rationales

ATH has been shown to inhibit serine proteases either at a similar or faster rate than non-covalent AT+UFH. (14) Furthermore, investigations performed in a rabbit jugular thrombosis treatment model demonstrated that ATH reduced clot mass by 17%, as opposed to an increase in the clot mass observed with the administration of UFH, AT+UFH or saline. (16) It was speculated that the observed decrease in clot mass was a result of the effective inhibition of clot-bound FIIa and simultaneous dissolution of the clot by endogenous Pn from the fibrinolytic system. However, it is unknown to what degree ATH interacts with the components of fibrinolytic pathway, and whether ATH may further enhance fibrinolysis.

It has been shown that Pn is susceptible to inhibition by AT+UFH. (3,4,94) Catalytic concentrations of UFH enhance AT mediated inhibition of Pn, apparently by a

conformational mechanism. (3,4). k_2 values for the inhibition of Pn by AT have been reported to be 10^4 - 10^5 M^{-1} min^{-1} in the absence of heparin and 10^6 M^{-1} min^{-1} in the presence of heparin. (3,4) Previous data have shown that ATH exhibits faster inhibition rates for those enzymes inhibited via the template-mediated inhibition mechanism. (14) Since Pn has been reported to be inhibited by a conformational mechanism (3) it was suspected that the rates of inhibition for Pn by ATH may be similar to those achieved by AT+UFH.

Evidence to date has demonstrated that heparin can have variable effects on tPA mediated generation of Pn. Studies have shown that heparin can inhibit (95), enhance (9,95-100) or have no effect (95,99,101) on the tPA mediated generation of Pn. The diversity of results may be a result of the variations in experimental procedures used in these studies. It was therefore necessary to clarify the effects that heparin may have on Pn generation. In this study, the rates of Pn generation were monitored in the presence of its cofactor fibrin, and the effects of UFH, AT+UFH and ATH were compared. Further, it is well known that surface-bound coagulation factors are protected from inhibition by AT+UFH. (90,91) In the present study, Pn has the potential to bind to fibrin(ogen). It has been demonstrated that ATH possesses a superior ability to inhibit surface-bound coagulation factors. (106,114-116) Thus, it was possible that ATH may inhibit Pn-bound fibrin to a greater extent than AT+UFH, thus inhibiting the rate of generation of Pn to a greater extent than non -covalent AT+UFH.

Similar to surface-bound coagulation factors, fibrin-bound Pn is protected from inhibition by its physiological inhibitor α_2-AP. (53) However, protection of fibrin bound Pn from inhibition by AT+UFH and ATH has not been studied before. Since we have

previously shown that UFH may form ternary complexes with fibrin and enzymes (87) to protect the enzymes from inhibition by AT+UFH, we further investigated potential effects of reacting excess UFH with ATH for inhibition of Pn. Additionally, it is accepted that inhibition of Pn by α_2-AP occurs in a two-step mechanism in which unavailability of the LBDs reduces the rate of inhibition (48,49,90). To determine if AT inhibits Pn by a similar mechanism; separate experiments were performed utilizing EACA, which can occupy the LBDs on Pn potentially reducing the rates of inhibition by AT.

Previous studies have demonstrated that GAG chains do not increase the activity of Pn directly, (98) rather the apparent affect may be due to the increase in tPA mediated Pn generation. (98) In the present study, the direct effects of UFH, AT+UFH and ATH were tested and compared using a fixed concentration of tPA.

1.12. Specific Objectives

1) To determine the mechanism of inhibition and highest k_2 values achieved by AT+UFH for Pn inhibition and compare these results to those achieved by ATH
2) To determine the effects of AT+UFH or ATH or UFH on Pn generation in the presence of an intact fibrin clot
3) To study potential protection of Pn by fibrin(ogen) from inhibition by AT+UFH compared to ATH
4) To study the potential mechanisms for the protection of Pn from inhibition by AT+UFH or ATH
5) To determine potential modulation of the chromogenic activity of tPA by AT+UFH or ATH or UFH

2. Experimental Procedure

2.1 Materials

2.1.1 Reagents

All reagents used were of analytical grade. Sodium chloride and Tris (tris (hydroxymethyl) amino-methane) were purchased from Bioshop (Burlington, ON). Polyethylene glycol 8000, calcium chloride dihydrate ($CaCl_2$), sodium lauryl sulphate (SDS), sodium phosphate (monobasic, monohydrate) were from BDH Inc. (Toronto, ON). Hexadimethrine bromide (Polybrene) was obtained from Aldrich Chemical Company Inc. (Milwaukee, WI). Tween 80 and epsilon aminocaproic acid (EACA) were from Sigma (St. Louis, MO, USA)

2.1.2 Heparin

UFH sodium salt from porcine intestinal mucosa was obtained from Sigma (St. Louis, MO, USA). Experimental tests involving UFH samples were sub-sampled from a single UFH stock of 10 mg/ml frozen in phosphate buffered saline (PBS) (0.016M Na_2HPO_4(anhydrous), 0.004M $NaH_2PO_4 \cdot H_2O$, 0.15M NaCl, pH 7.3)

2.1.3 Enzyme Substrates

S-2366 substrate for activated protein C and XIa (L-pyroglutamyl-L-prolyl-L-arginine-p-nitroaniline hydrochloride), S-2288 (H-D-isoleucine-proline- arginine-p-nitroaniline dihydrochloride), substrate for tPA and a broad spectrum of other serine proteases, and S-2251 (H-D-Valyl-L-leucyl-L-lysine-p-nitroaniline dihydrochloride) substrate for Pn were obtained from Diapharma (West Chester, OH, USA).

2.1.4 Proteins

Human AT (lot PR06-0046R1) was purchased from Affinity Biologicals (Ancaster, ON, Canada). Human coagulation proteins, Pn, Glu-Pg and Pg, Von Willebrand factor and fibronectin depleted fibrinogen were supplied by Enzyme Research Laboratories (South Bend, USA). Two chain r-tPA (tc r-tPA) was supplied from American Diagnostica (Stamford, CT, USA). Viprinex (Ancrod, lot # 901463) was supplied by Neurobiologicals and produced by Baxter Pharmaceuticals (Deerfield, IL, USA). ATH was produced according to the procedures previously described. (105) For all experiments, ATH was used from lot #010914.

2.2 Methods

2.2.1 Determination of Protein Purity

Glu - Pg, Pn, fibrinogen as well as inhibitors AT and ATH, were analyzed for purity by sodium dodecyl sulphate polyacrylamide gel electrophoresis (SDS-PAGE) under reducing and non-reducing conditions. 10 µg of Pn, AT and ATH and 0.25 µg of Glu -Pg, fibrinogen, and 10 U/ml of Ancrod were each prepared in a final volume of 15 µL inclusive of the sample buffer (diluted in PBS buffer). These samples were heated at 100^{o}C for five minutes and loaded into the wells of a polyacrylamide gel (4% stacking and 7.5% or 12% separating polyacrylamide gel). The gel was electrophoresed at 200 V until the dye front approached the bottom of the gel. After electrophoresis, the gel was removed, fixed and subjected to Alcian Blue and Coomassie Brilliant Blue R250 staining and destaining or subjected to silver staining using ProteoSilver ^{TM} Silver Stain Kit

(Sigma, St. Louise , Missouri) following the instructions provided by the manufacturer. Gels were then dried using a BioRad gel dryer.

2.2.2 Analysis of Pn degradation using SDS-PAGE

Due to the autocatalytic nature of Pn, it was necessary to evaluate the changes which occur in the structural properties of Pn over a period of time. To do this a diluted sample of Pn (3000 nm) was incubated at room temperature for a period of 24 hours. Subsequently, samples of 2.5 µg were taken at intervals of 0, 0.5, 1, 1.5, 2, 2.5, 3, and 24 hours. Each sample was diluted with PBS buffer for a final volume of 15 µL inclusive of the sample buffer. Samples were then subjected to electrophoresis as described above for 40 min at 200 V. (4% stacking and 12% separating polyacrylamide gel) After electrophoresis, the gel was removed, fixed and subjected to silver staining using ProteoSilver ^{TM} Silver Stain Kit (Sigma, St. Louise , Missouri) following instructions provided by the manufacturer. The Gel was then dried using a BioRad gel dryer.

2.2.3 Detection of inhibitor-enzyme complexes using SDS-PAGE

To detect the formation of enzyme-inhibitor complexes, samples containing 2.5µg of Pn were incubated at room temperature with 1.5µg of AT+50,000 nM UFH or 1.5 µg of ATH. Pn:inhibitor molar ratio was 1:1. Samples were then subjected to electrophoresis as described above for 40 min at 200 V. (4% stacking and 7.5% separating polyacrylamide gel) After electrophoresis, the gel was removed, fixed and subjected to silver staining using ProteoSilver ^{TM} Silver Stain Kit and dried as above.

2.2.4. Titration of Plasmin with inhibitors AT+UFH and ATH

Inhibition of Pn by inhibitors AT+UFH and ATH was determined by incubation of 10 µL of 60 nM of Pn with 10 µL of increasing concentrations of the inhibitors AT+UFH (AT:UFH=1:1) or ATH for a period of 15 min in TSP + $CaCl_2$ buffer (20 mM Tris, 150 mM NaCl, 0.6% polyethylene glycol 8000, 2.5 mM $CaCl_2$, pH 7.4) at room temperature. Inhibitor:enzyme ratio ranged from 0-8. After incubation of enzyme with inhibitor, reactions were neutralized by the simultaneous addition of 80 µL of solution containing 1.25 mg/mL of polybrene and 0.5 mM of the Pn substrate S-2366 in TSP. The residual enzyme activity was continuously measured at an absorbance of 405 nm using a SpectraMax Plus 384 plate reader (Molecular Devices, Sunnyvale, CA, USA) for 10 min. Percent enzyme activity (V_t/V_o) was then plotted against the ratio of inhibitor:enzyme tested.

2.2.5 Determining the highest k_2 values for inhibition of Pn by AT+UFH

Discontinuous second order rate constant assays were performed to determine final k_2 values for inhibition of free Pn by AT and varying concentrations of UFH, as previously described.(14) A minimum inhibitor:enzyme ratio of 10:1 was maintained for all reactions. Briefly, 10 µL of 20 nM Pn was placed in 6 separate wells of a 96-well flat bottom microtiter plate (Fisher, Nepean, ON, Canada) at 37^o C. At specific time intervals (60 or 480 sec), 10µL of 200 nM AT + 0-10,000 nM UFH was added to the first 5 wells of the plate, while buffer was added to the last well as the control (uninhibited Pn). Enzymes, inhibitors and UFH were all diluted in TSP buffer + $CaCl_2$. The final concentrations of reactants were: 10 nM Pn, 100 nM AT, 0-5000 nM UFH and 2.5 mM

$CaCl_2$. After an additional time interval, reactions were terminated by the simultaneous addition of 80 µL of solution containing 1.25 mg/mL of polybrene and 0.5 mM of the Pn substrate S-2366 in TSP (20 mM Tris, 150 mM NaCl, 0.6% polyethylene glycol 8000, pH 7.4) The residual enzyme activity was continuously measured at an absorbance of 405 nm using a SpectraMax Plus 384 plate reader (Molecular Devices, Sunnyvale, CA, USA) for 10-30 min. Pseudo first order rate constants (k_1) were calculated by determining the negative slope of the line from plots of ln V_t/V_o versus the inhibition time, where V_o is the uninhibited enzyme activity at time t=0 and V_t is the residual enzyme activity at time t. The k_2 values were calculated by dividing the k_1 by the concentration of inhibitor used. Final k_2 values were calculated from the average of 5 separate experiments.

2.2.6. Pn generation in the presence of an intact fibrin clot

Pn was generated using modifications of the methods of Schneider et al. (53) and Kim et al. (118). In our study, rates of Pn generation were measured in the presence of an intact Ancrod-generated fibrin clot formed in wells of a 96-well plate. Briefly, Pn generation and fibrin polymerization were initiated by the simultaneous addition of 90 µL of a solution containing fibrinogen (1µM), Glu-Pg (0.4 µM), S-2251 (400 µM) and $CaCl_2$ (2.5 mM) to wells containing 5 µL of 0.6 U/ml of Ancrod and 5 µL of 0.0625 nM tPA in TBS-T80 (50 mM Tris-Cl pH 7.4, 0.1 M NaCl, 0.01% Tween 80) at 37^{o}C. Ancrod is a FIIa-like serine protease which cleaves fibrinopeptide A (FpA) from the α chain of the fibrinogen molecule, but not fibrinopeptide B, exposing only two polymerization sites on each fibrin monomer thus inducing a relatively weak polymerization of fibrin compared to FIIa. (119) Reactions were initiated in the presence of AT+UFH (1:1), UFH alone or ATH at concentrations ranging from 0-1000 nM. After initiation, absorbance was

monitored at two separate wavelengths, 405 and 450 nm. The 405 nm is a composite of S-2251 hydrolysis by Pn and changes in turbidity associated with clot formation. Changes in absorbance at 450 nm reflect only the turbidity produced by fibrin polymerization. The rates of Pn generation were calculated as previously described and are described below. (120) Absorbance values which reflect hydrolysis of the substrate S-2251 only, (A_{corr}) were determined by subtracting the absorbance measurements at 450 nm from the readings obtained at 405 nm according to the relationship $A_{corr} = A_{405} - (CF \times A_{450})$. The readings at 450nm were multiplied by a correction factor (CF) which was determined by forming a fibrin clot in the absence of tPA, to correct for the turbidity at 450nm. Subsequently, according to the relationship $A_{corr} = (SA \times r/2) \times t^2$ where SA is the specific activity of Pn against S-2251 in the presence of a 1 µM fibrin clot, *r* is the rate of Pn generation and *t* is time, corrected absorbance values were plotted against t^2 to determine slopes (SA x *r/2*) of the linear plots generated. The rates were then calculated using SA which was experimentally determined to be 0.66 A_{corr}/min/µM in the presence of a 1 µM fibrin clot. Rates (sec^{-1}) were then plotted against the concentration of the anticoagulant tested.

2.2.7 Detection of FDPs from Pn generation assays using SDS- PAGE

Since FDPs can also potentiate Pn generation, SDS-PAGE was utilized to detect the formation of FDPs in the assays preformed in section 2.2.6. Reaction volumes of 20 µL were prepared in Eppendorff tubes at room temperature utilizing the same concentrations of proteins in section 2.2.6. To observe the formation of FDPs over time, 5 separate reactions were initiated simultaneously and terminated at specific time intervals (2, 12, 20, 40 and 100 min) by the addition of 20 µL sample buffer containing β-

mercaptoethanol and sodium dodecyl sulphate for a final volume of 40 µL. These samples were immediately heated at 100^{o}C for 5 min. Next, 20 µL of the reaction + sample buffer mixture was loaded into the wells of a precast polyacrylamide gradient gel (4% stacking and 15% separating) (Mini-PROTEAN TGX, Bio Rad Laboratories, Mississauga, Ontario) after the termination of the last reaction. The loaded sample contained 3.3 µg of Fg, 0.72 µg of Pg, 0.6 U/ml of Ancrod and 0.689 pg. Samples were then subjected to electrophoresis for 40 min at 200 V. After electrophoresis, the gel was removed, fixed and subjected to silver staining using ProteoSilver ^{TM} Silver Stain Kit (Sigma, St. Louise , Missouri) following instructions provided by the manufacturer. The Gel was then dried using a BioRad gel dryer.

2.2.8 Determination of k_2 values for inhibition of Pn with or without fibrin(ogen) by AT+UFH or ATH

Discontinuous second order rate constant assays were performed as above to compare k_2 values obtained here to those obtained for the inhibition of free Pn by AT+UFH versus ATH. From our previous data above, we have established that the concentration of UFH required to achieve the highest inhibition rates for inhibition of 10 nM Pn by 100 nM AT was 3000 nM UFH. Therefore, for any subsequent investigations utilizing AT+UFH, the final concentration was 100 nM AT+3000 nM UFH. For ATH reactions, we utilized 100 nM ATH. The k_2 values for both AT+UFH and ATH were calculated as above.

For inhibition rate experiments utilizing fibrin, the procedure was performed as follows: 200 nM of fibrinogen and 0.6 U/mL of Ancrod in TSP buffer + Ca_2Cl was reacted for 15 min at room temperature. At this concentration the formed fibrin monomer

does not polymerize. Next a concentrated solution of Pn (3 µM) was added to the fibrin + Ancrod solution (to give 20 nM Pn). Ten µL of the fibrin monomer/Ancrod/Pn solution was then added to 6 wells of a 96-well plate, followed by addition of appropriate inhibitors as described above. Final concentrations of reactants were: 10 nM Pn, 100 nM AT, 3000 nM UFH, 100 nM fibrin and 2.5 mM $CaCl_2$. For inhibition rate experiments with purified fibrinogen, 100 nM of fibrinogen alone was included with Pn and inhibitors.

2.2.9 Detection of FPA release from fibrinogen

In order to confirm the release of FPA from the α chains of fibrinogen by reaction with Ancrod a competitive enzyme linked immunosorbent assay (ELISA) was performed using a kit from Diapharma (Westchester, OH) according to the instructions provided by the manufacturer. Steps were performed at room temperature unless otherwise indicated. Briefly, fibrin was prepared by incubation of 200 nM of purified fibrinogen with 0.6 U/ml of Ancrod for a period of 15 min. Additional samples were prepared containing fibrinogen and Ancrod only as controls. Samples were then treated with Bentonite to remove un-reacted and therefore possibly cross-reactive fibrinogen by the addition of 0.5 ml of the Bentonite solution to 1 ml of samples. Samples were then centrifuged for 20 min using a micro-centrifuge. Subsequently 1 ml of the supernatant was collected and Bentonite absorption was repeated as above followed by the removal of 1 ml of the supernatant which was used as the sample. The samples containing FPA were then diluted to 1:80 to bring the concentration of FPA within the range of the standard curve. Standards were prepared using the FPA calibrator provided with the kit which had a starting concentration of 55 ng/ml after reconstitution. Serial dilutions ranging from 1:1

to 1:64 were then made and used to construct a standard curve. Aliquots of human affinity-purified rabbit antibody were then added to each of the samples and the standards and were allowed to incubate for a period of 1 h at 37 ^{O}C to allow binding of antibody to FPA. Next, aliquots of the samples and standards were then added to wells of a micro-titer plate pre-coated with synthetic FPA by the manufacturer and allowed to incubate for a period of 1 hour. Next, 5 successive washes were made using washing buffer followed by the incubation of anti-rabbit IgG polyclonal antibody coupled with horse radish peroxidase (HRP) for a period of 1 h. Following incubation, an additional 5 successive washes were then preformed as above. Immediately after washing a peroxidase substrate was added to the wells (3,3',5,5' Tertramethylbenzidine (TMB), containing hydrogen peroxide) and allowed to develop for 300 sec. The reactions were then terminated by the addition of 0.45 M sulfuric acid. Absorbance readings were then measured at 450 nm. Absorbance values were then plotted against the FPA concentration to generate a standard curve. The FPA concentrations in the samples were then determined using the curve obtained and values multiplied by 2 to correct for a two-fold dilution of the samples during treatment with Bentonite. Lastly, the values were multiplied by 80 to correct for the dilution of the original sample to obtain final FPA concentrations.

2.2.10 Studies of the mechanism for the protection of Pn

Since we have previously shown that UFH may form ternary complexes with fibrin and enzymes (106) to protect the enzymes from inhibition by AT+UFH, we further investigated potential effects of adding excess UFH with ATH on inhibition of Pn. Briefly, 3000 nM UFH and 100 nM ATH was reacted at 37^{o}C with 10 nM Pn as described above, and the final k_2 values were determined.

To assess if the occupation of LBDs of Pn are involved in its protection from inhibition by AT+UFH or ATH, additional inhibition assays were repeated as above, however Pn was incubated with a 10-fold molar excess of EACA prior to reaction with inhibitors to occupy LBDs on plasmin.

2.2.11 Assays for chromogenic activity of tPA

To investigate the potential interactions of tPA with UFH, AT+UFH and ATH, aliquots of tPA were titrated with increasing concentration of the individual reagents. Increasing concentrations of UFH, AT+UFH or ATH were incubated with 20nM of tPA in wells of a 96 flat bottom plate for a period of 15 min in TBS-T80 at room temperature. The concentrations of the various reagents were at inhibitor:tPA molar ratios ranging from 0 to 20:1. Reactions containing UFH or ATH were neutralized by simultaneous addition of a solution containing either 1.25 mg/ml of polybrene and tPA substrate, S-2288 in buffer. Enzyme activity was then determined by measuring the rate of substrate cleavage (Vmax) for 10 min using a plate reader. Vmax values were then expressed as percentages of the uninhibited enzyme activity and plotted against the molar ratios of the inhibitor and tPA tested.

2.2.12 Statistical analysis

Data were expressed as mean ± SEM ($n \geq 5$) to measure the variability of the resutls. Additionally taking an average of at least 5 tests allows reporting of accurate and more precise data. Tests of comparisons between two groups were measured using a two-tailed student's t-test and multiple groups were measured by ANOVA. Values of $p<0.05$

were considered significant. Final plots were generated used Sigma Plot 11.0. (San Jose, California). Statistical analysis was done using GraphPad Prism. (La Jolla, California)

3. Results

3.1 Protein purity

Purity of some of the purified proteins used in this study was assessed by SDS-PAGE. (Figure 6 and 7) Figure 6 shows a single band appearing at ~ 59 kDa representing AT in lane 2. Lane 3 shows a smear of higher molecular weight (MW) which represents the ATH molecules. A single band appears at ~59 kDa which represents the free AT in the ATH preparation, a faint smear at low MW in lane 3 represents residual free UFH in the preparation. Lane 4 shows Pn under reducing conditions. Bands appear at ~100 kDa, a strong band between ~75 and 63 kDa, a faint band at ~48 kDa, a second strong band at ~26 kDa and a faint band at ~12 kDa. The heavy chain of Pn has a molecular weight of ~57 kDa and the light chain of Pn has a MW of ~26 kDa which are represented by the two most prominent bands. The band appearing at ~48 may represent the uPA which was used to activate Pg and which was not removed from the preparation according to the manufacturer. The band appearing at ~12 kDa likely represents the activation peptide which is released following activation of the Pg molecule. Lane 5 shows Pn under non-reducing conditions. A single band appears at ~83 kDa which represents the full two chain Pn molecule. A faint band appears at ~ 48 kDa which may represent the uPA used to activate Pg in the production of the enzyme by the manufacturer.

Figure 7 shows SDS-PAGE of Pg, fibrinogen and Ancrod. Lane 2 shows a single band at ~ 90 kDa representing Pg. Lane 4 shows the α- chain of fibrinogen at ~70 kDa, β-

chain at ~60 kDa and the γ-chain at ~55 kDa. Lane 5 shows a single band ~ 48 kDa representing Ancrod a single chain highly glycosylated protein. (121) Two chain r - tPA was not visualized as a single band due to the presence of a relative excess of bovine serum albumin in the stock supplied by the manufacturer used as a stabilizing agent. (gel not shown)

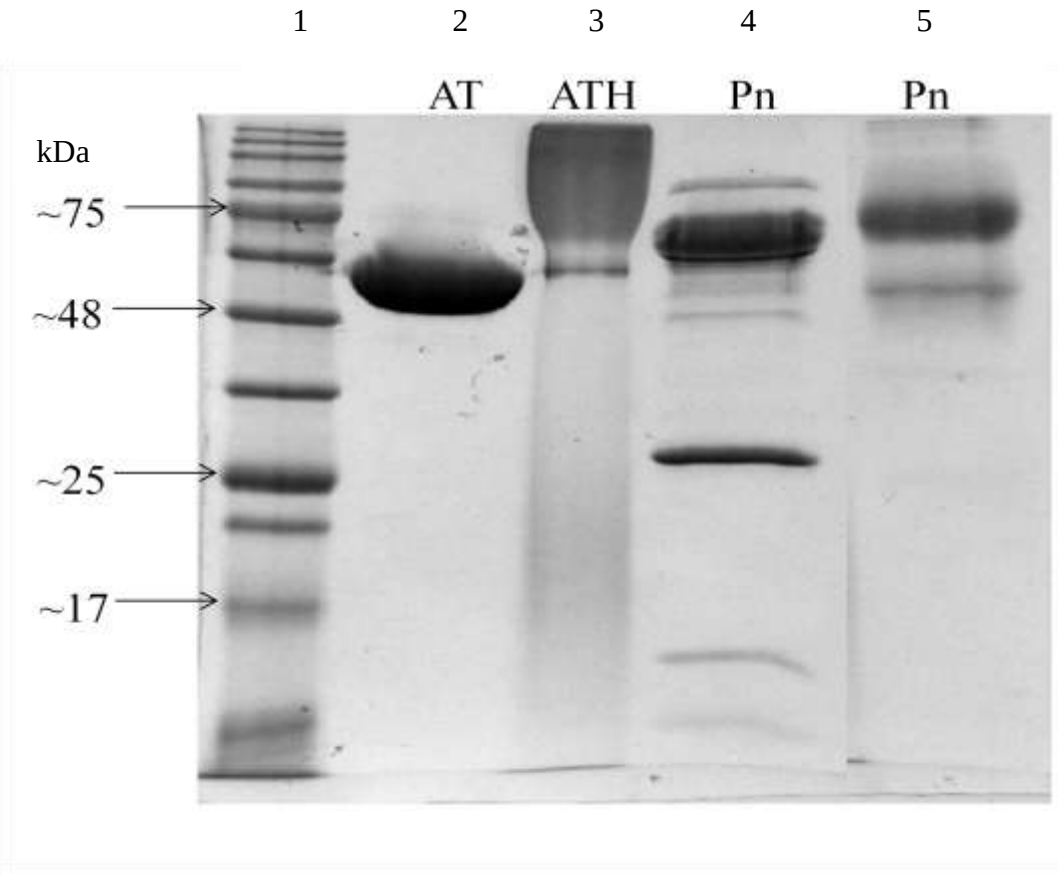

Figure 6. SDS-PAGE of AT, ATH and plasmin

Electrophoresis was performed under reducing and non-reducing conditions in a discontinuous, (12% separating and 4% stacking) polyacrylamide gel. After electrophoresis of the denatured proteins and their fixation, the proteins were stained with Coomasie brilliant blue R250 dye. GAGs were stained with Alcian Blue. In this gel, Lane 1 represents BLUeye pre-stained protein ladder, Lane 2 represents 10µg AT (59kDa), Lane 3 represents 10µg ATH , Lane 3 represents 10µg Pn enzyme under reducing conditions (HC - 57 kDa; LC – 26 kDa), Lane 4 represents 10µg Pn enzyme under non-reducing conditions (83 kDa)

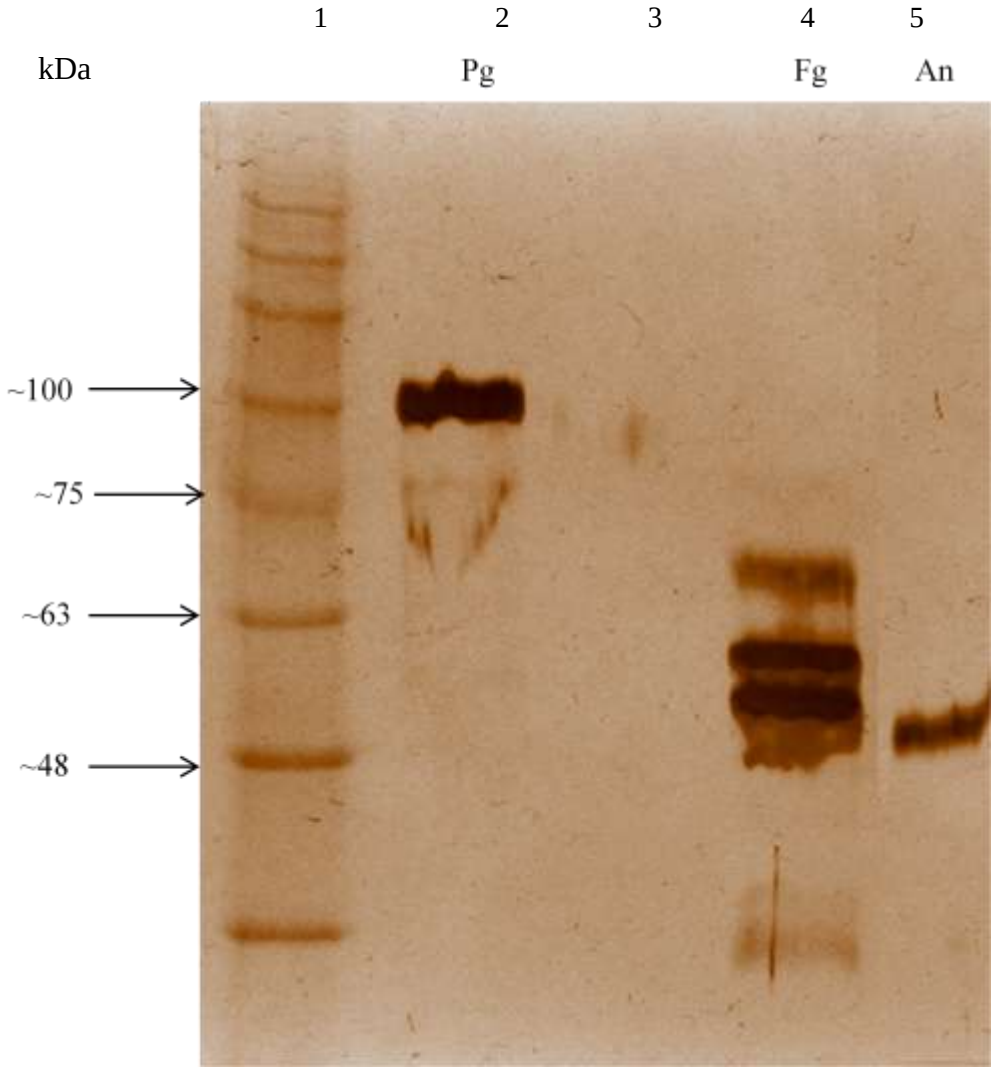

Figure 7. SDS-PAGE of plasminogen, fibrinogen and Ancrod

Electrophoresis of proteins was performed under reducing conditions in a discontinuous gel (7.5% separating and 4% stacking gel). The proteins were stained with ProteoSilver ™ Silver Stain Kit. Lane 1 represents BLUeye pre- stained protein ladder, Lane 2 represents 0.25 µg Glu - Pg (Pg) (90 kDa), Lane 3 is blank, Lane 4 represents 0.25 µg Fibrinogen (Fg) (α chain - 63 kDa, β chain - 56 kDa, γ Chain - 47 kDa), Lane 5 represents 10 U/ml of Ancrod (37 kDa).

3.2 Analysis of Pn degradation using SDS-PAGE

Figure 8 shows SDS-PAGE analysis of Pn degradation. Samples of Pn were taken at specified intervals and subjected to electrophoresis. Bands are similar to those described for the SDS-PAGE analysis of Pn above. No new bands appear as the incubation period increases. A decrease in band intensity is only observed after ~24h of incubation at room temperature.

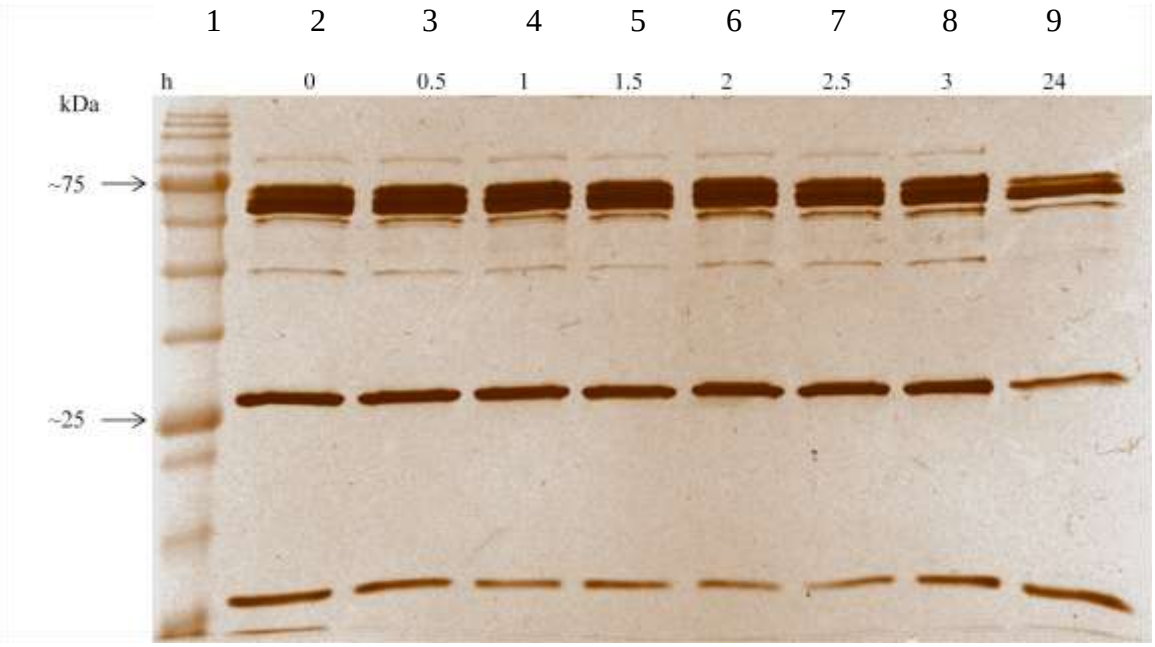

Figure 8. SDS-PAGE of plasmin degradation over a period of 24h

Subsamples were removed at the indicated times (hours) from a sample of Pn kept at room temperature. Electrophoresis of the subsample was performed under reducing conditions in a discontinuous gel (12% separating and 4% stacking gel). The protein was stained with ProteoSilver ^{TM} Silver Stain Kit. Lane 1 represents BLUeye pre- stained protein ladder. Lanes 2-9 represent subsamples of Pn containing 2.5 µg of protein.

3.3 Detection of inhibitor-enzyme complexes using SDS-PAGE

SDS-PAGE was utilized to detect the formation of Pn-inhibitor complexes following reaction of Pn with AT+UFH or ATH. Figure 9 shows formation of high molecular weight complexes in lanes 6 and 8 for Pn-AT and Pn-ATH respectively, confirming covalent linkage between inhibitor and enzyme. The expected size of the Pn-AT complex is 142 kDa, (AT (59 kDa) and Pn (83 kDa)). The sizes of Pn+ATH complexes are expected to be a heterogeneous mixture with a broad range due to the heterogeneity of the UFH chains, in terms of MW, of the ATH molecules. The range of ATH molecules has been reported to be 69 – 100 kDa. (105) (Fig. 6)

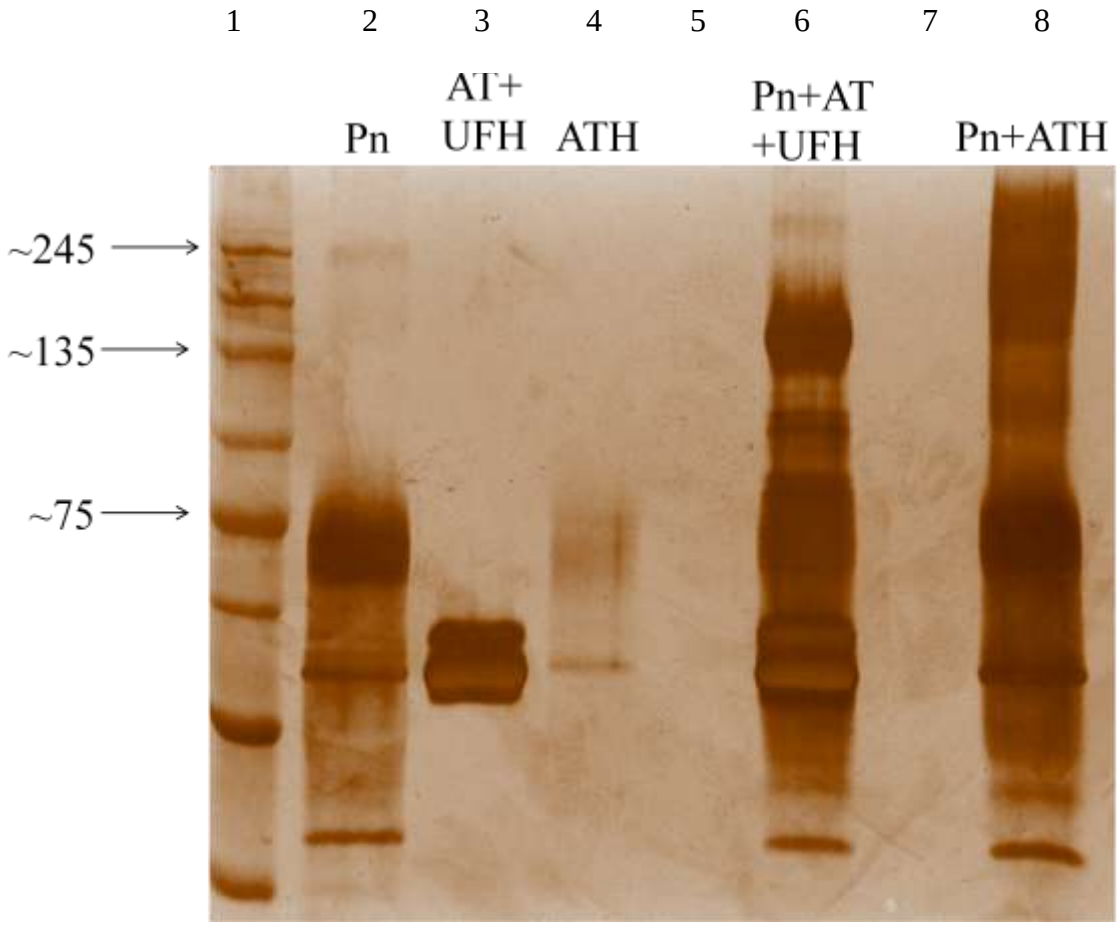

Figure 9. SDS-PAGE of Plasmin+AT+UFH and Plasmin+ATH reactions

Electrophoresis of enzyme and inhibitor was performed under non-reducing conditions in a discontinuous gel (7.5% separating and 4% stacking gel). The protein was stained with ProteoSilver ™ Silver Stain Kit. Lane 1 represents BLUeye pre- stained protein ladder. Lane two represents 2.5 µg of Pn, Lane 3 represents 1.5 µg of AT+ 2.25 µg of UFH, Lane 4 represents 1.5 µg of ATH, Lane 5 blank, Lane 6 represents 2.5 µg of Pn + 1.5 µg of AT+50,000 nM UFH, Lane 7: Blank; Lane 8 represents 2.5 µg of Pn+ 1.5 µg of ATH; incubation time for reactions was 15 min

3.4 Determining the mechanism of inhibition and highest k_2 values for Pn inhibition by AT+UFH

Pn was first titrated with inhibitors AT+UFH and ATH to determine Inhibitor:enzyme ratio required to produce maximal inhibition of enzymatic activity. Enzymatic activity was greatly reduced at ratios of 2:1 and at ratios of 8:1 >98% inhibition was observed. (Figures 10,11) Second-order rate constant (k_2) assays were performed to determine and compare the k_2 values for the inhibition of free Pn by AT and varying levels of UFH. When 10 nM Pn was inhibited by 100 nM AT alone, k_2 values of $2.82x10^5 \pm 0.45x10^5$ $M^{-1}min^{-1}$ were observed. The k_2 values increased with addition of successively higher concentrations of UFH until a plateau was reached. The maximal k_2 value was $5.74x10^6 \pm 0.28x10^6 M^{-1}min^{-1}$ at a UFH concentration of 3000 nM. No significant changes in the k_2 values were observed after the addition of higher concentrations of UFH which suggests that Pn is inhibited by a conformational mechanism. (figure 12)

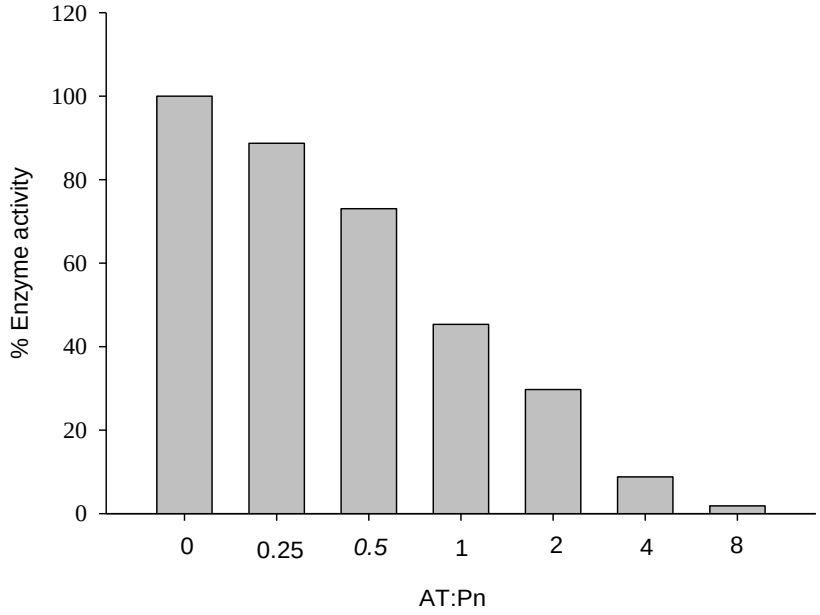

Figure 10. Titration of free Pn with AT+UFH

Sixty nM Pn was incubated with increasing concentrations of AT+UFH (1:1) for a period of 15 min. Following incubations, reactions were neutralized by the addition of a solution containing 1.25 mg/mL of polybrene and 0.5 mM of the Pn substrate S-2366 in TSP buffer with 2.5 mM $CaCl_2$. Remaining enzymatic activity was then determined by reading absorbance with a plate reader.

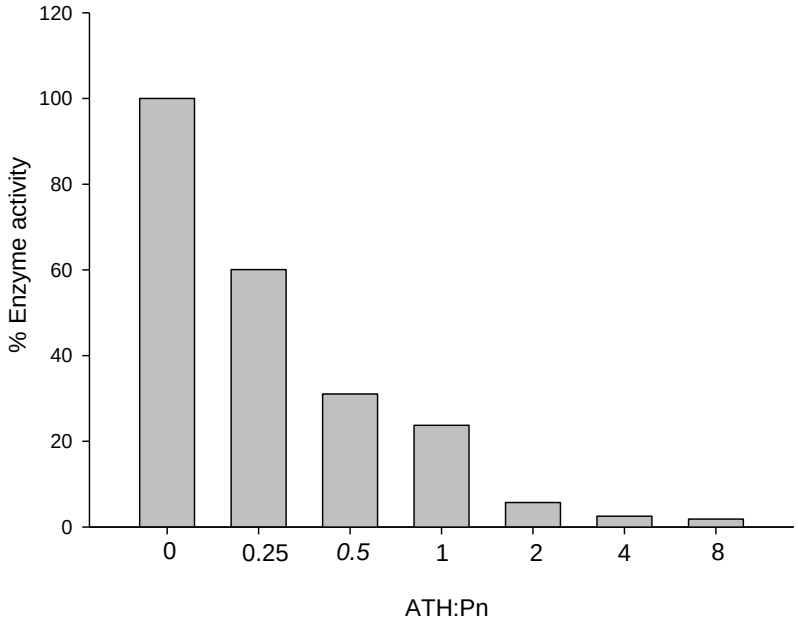

Figure 11. Titration of free Pn with ATH

Sixty nM Pn was incubated with increasing concentrations of ATH for a period of 15 min. Following incubations, reactions were neutralized by the addition of a solution containing 1.25 mg/mL of polybrene and 0.5 mM of the Pn substrate S-2366 in TSP buffer with 2.5 mM $CaCl_2$. Remaining enzymatic activity was then determined by reading absorbance with a plate reader.

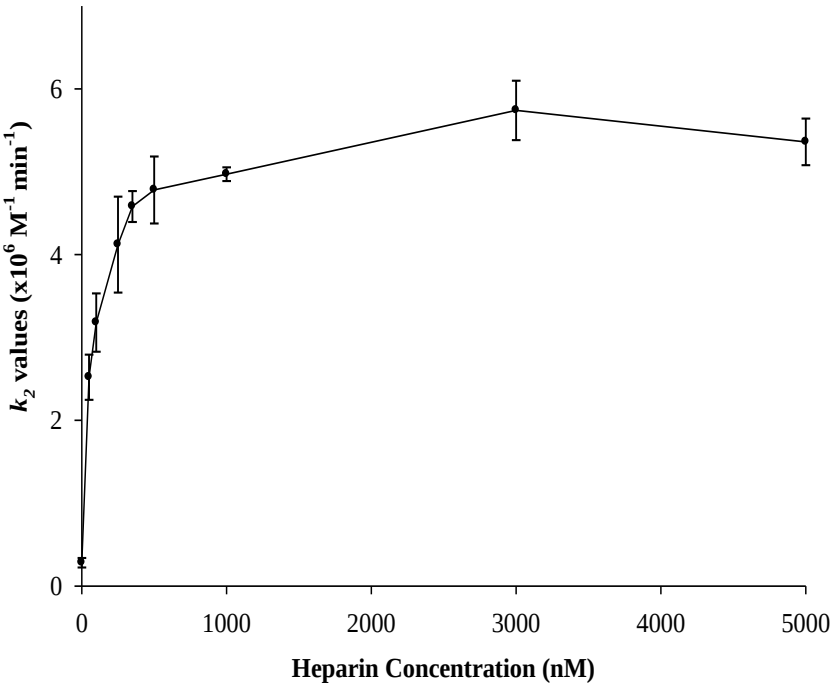

Figure 12. Inhibition of free Pn by AT+UFH

Second-order rate constants (k_2 values) were measured under pseudo first-order conditions in the presence of 2.5 mM of $CaCl_2$. The Pn concentration was 10 nM, AT concentration was 100 nM, and UFH concentrations ranged from 0 – 5000 nM. The k_2 values are an average of n=5 ± standard error of mean

3.5 Determination of the rates of Pn generation in the presence of a fibrin clot

Since FIIa is inhibited by AT + UFH, Ancrod was used as an alternate fibrin polymerizing agent in its place. A concentration of 0.6U/ml of Ancrod was found to be sufficient to induce fibrin polymerization such that changes in absorbance at both 405 nm and 450 nm would be detectable during readings.(figure 13) This concentration of Ancrod also resulted in fibrin polymerization early in the assay making fibrin available for Pn degradation. Further it was established that Ancrod was not inhibited by AT+UFH or ATH and that Ancrod does not cleave the substrate S-2251. (data not shown).

3.5.1 Determination of Pn specific activity

The specific activity of Pn was determined by reacting known concentrations of Pn, ranging from 0-10 nM, with the substrate S-2251 in the presence of a 1 μM fibrin clot. Absorbance changes were then monitored in a SpectraMax Plus 384 spectrophotometer. The Vmax values (mOD/min) were plotted against Pn concentrations and the slope of the line of best fit was determined. (figure 14) The specific activity was found to be 0.66 A_{corr}/min/μM with a $r^2 = 0.97$. This value was be used to determine the rate of Pn generation according to the relationship: $A_{corr} = (SA \times r/2) \times t^2$.

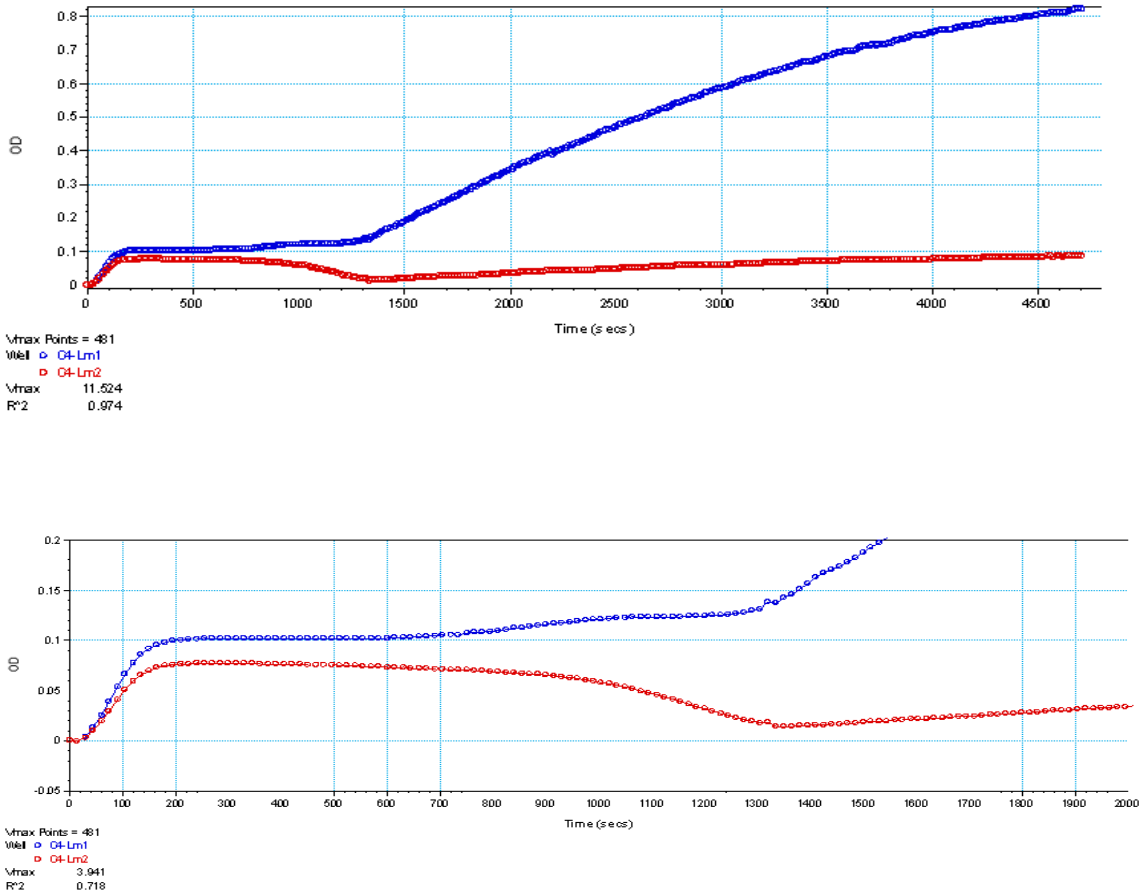

Figure 13. Example of readings showing clot formation and lysis

Clot formation is essentially complete at around 200 seconds and clot lysis is being initiated at 1000s with readings returning to baseline by 2500s. Clot formation and Pn generation was initiated by the simultaneous addition of 1µM fibrinogen, 0.4 mM S-2251, 0.4 µM Glu – Pg to wells containing 0.6 U/ml Ancrod and 0.0625 nM tPA. The Blue curves reflects absorbance changes at 405 nm which represents a combination of S-2251 substrate hydrolysis and turbidity produced by fibrin, the red curve reflects absorbance changes at 450 nm which represents the turbidity changes produced by fibrin only

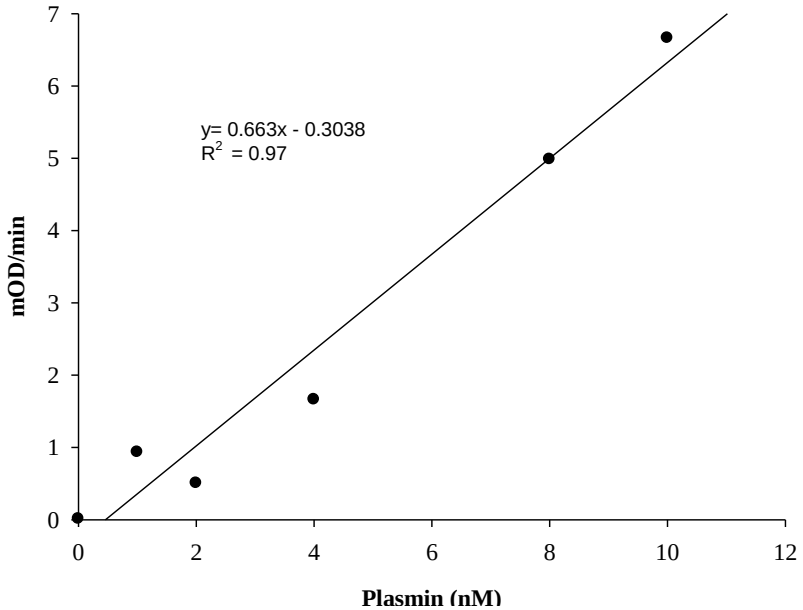

Figure 14. Standard curve for Pn specific activity

Various concentrations of Pn (0-10nM) were reacted with the Pn substrate S-2251 in the presence of a 1µM fibrin clot. Reactions were read at a 405nm using a plate reader. Pn specific activity was determined by taking the slope of the plot obtained

3.5.2 Calculation of the rates of Pn generation

To study the effects of UFH, AT+UFH, and ATH on fibrinolysis, we determined the rates of tPA-induced Pn generation in the presence of an intact fibrin clot, in the absence or presence of these anticoagulants. The methods used were similar to those of Kim *et al.* (118) in which FIIa is used to cleave purified fibrinogen to form a fibrin clot, which then serves to enhance tPA reaction with Pg. This intact fibrin clot is more physiologically relevant than the soluble fibrin substitutes that have been previously used in published studies investigating Pn generation. In our study, we used Ancrod instead of FIIa to form the fibrin clot since FIIa would consume the inhibitors AT and ATH.

The rates of Pn generation were plotted against the concentrations of UFH, AT+UFH or ATH tested. Results show that there was a reduction in the rates of Pn generation when either AT+UFH or ATH was present, with ATH producing a more pronounced reduction than AT+UFH (figure 15). Even at the lowest concentration of ATH tested, there was greater than 15-fold reduction in the rates of Pn generation compared to UFH or AT+UFH. For experiments utilizing UFH, it was observed that the rate of Pn generation was not altered even at the highest concentration tested.

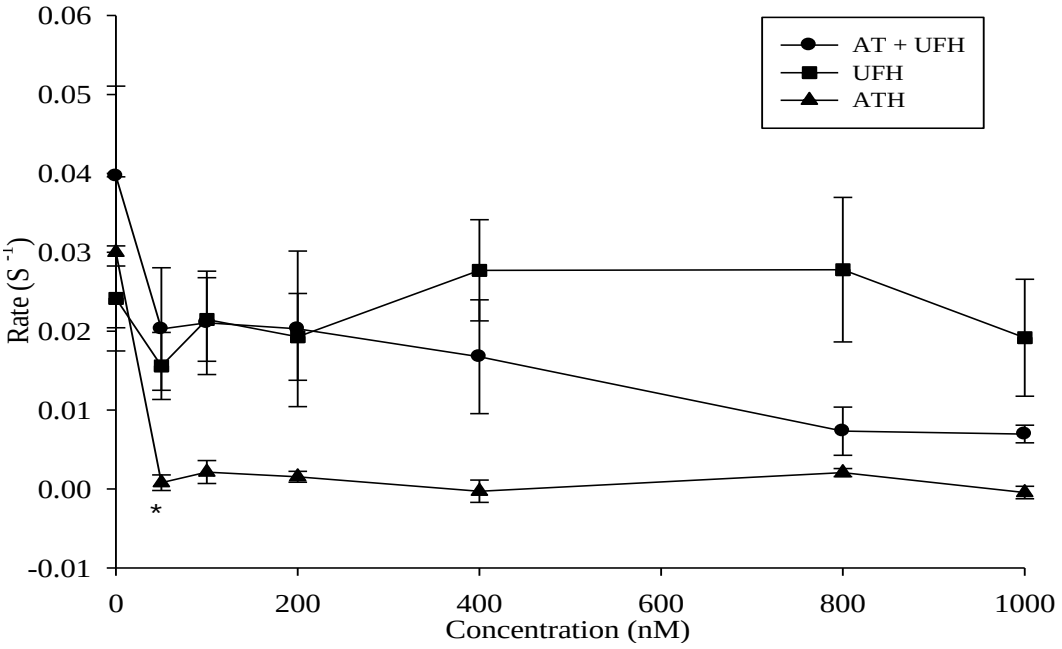

Figure 15. Rates of Pn generation in the presence of fibrin and either inhibitor AT+UFH or ATH or UFH alone

Rates of Pn generation were assessed using a combinational turbidometric and chromogenic assay measuring fibrin clot formation at 450 nm and cleavage of S-2251 by generated Pn at 405 nm, in the presence or absence of varying levels of inhibitors. Reactions were initiated by the addition of a mixture containing fibrinogen (1µM), Glu-Pg (0.4 µM), S-2251 (400 µM) and $CaCl_2$ (2.5 mM) in the presence of the inhibitors at the concentrations indicated, to wells containing 5 µL of 0.6 U/ml of Ancrod and 5 µL of 0.0625 nM tPA in TBS-T80. Rates of Pn generation were calculated as described in the materials and methods. Data is the average of n=5 ± standard error of mean. (*$p<0.001$)

3.6 Detection of FDPs in plasmin generation assays using SDS-PAGE

Studies have shown that FDPs can potentiate Pn generation by providing C-terminal Lys residues for binding of Pg and tPA. (122) To demonstrate the production of FDPs in the Pn generation assays in section 3.6, identical reaction mixtures were incubated for specific time periods and then subjected to SDS-PAGE under reducing conditions. The reaction mixtures contained 3.3 µg of Fg, 0.72 µg Pg, 0.689 pg of tc- tPA and 0.6 U/ml of Ancrod. (figure 16). Lane 2 of the gel shows the α (63 kDa), β (56 kDa) and γ chains (47 kDa) of fibrinogen. A faint band appears above the α chain at approximately 130 kDa which may represent α_2-AP (67 kDa) covalently linked to the α chain of the fibrinogen molecule. It has been determined that 1.2-1.8 moles of α_2-AP have are covalently linked per mole of mole of Fg. (123). Lanes 5-9 show bands at the α (63 kDa), β (56 kDa) and γ chains (47 kDa) of fibrinogen, a strong band appears at ~100 kDa which most likely represents Pg. Faint bands begin to appear at the ~25 kDa marker at 12 min, which most likely represent the light chain of Pn (26 kDa) which has been generated by tPA cleavage of Pg. This faint band increases in density as the reaction progresses and then decreases significantly in density at 100 min, most likely as result of proteolytic auto degradation. At the lowest portion of the gel, a faint band begins to appear which most likely represents the FPA which has been cleaved from the α chain of the fibrinogen molecule by Ancrod. This band increases in density as the reaction progresses, consistent with further clot formation. At ~35 kDa a faint band begins to appear which mostly likely represents fibrin degradation products. This may tentatively be the αC chain which has been cleaved off of the fibrinogen molecule, which has been reported to be cleaved by Pn to form fragment X. (123) Interestingly, changes in the

density of the bands representing fibrinogen chain occur at 100 min with a corresponding appearance of a band at the lowest portion of the lane which most likely are small FDPs produced late in the reaction. The appearance of the small FDPs correspond with an increase in the absorbance at 405 nm in the Pn generation experiments which can be seen in figure 13, which is mostly likely a result of the potentiating effect of the FDPs on Pn generation. (122)

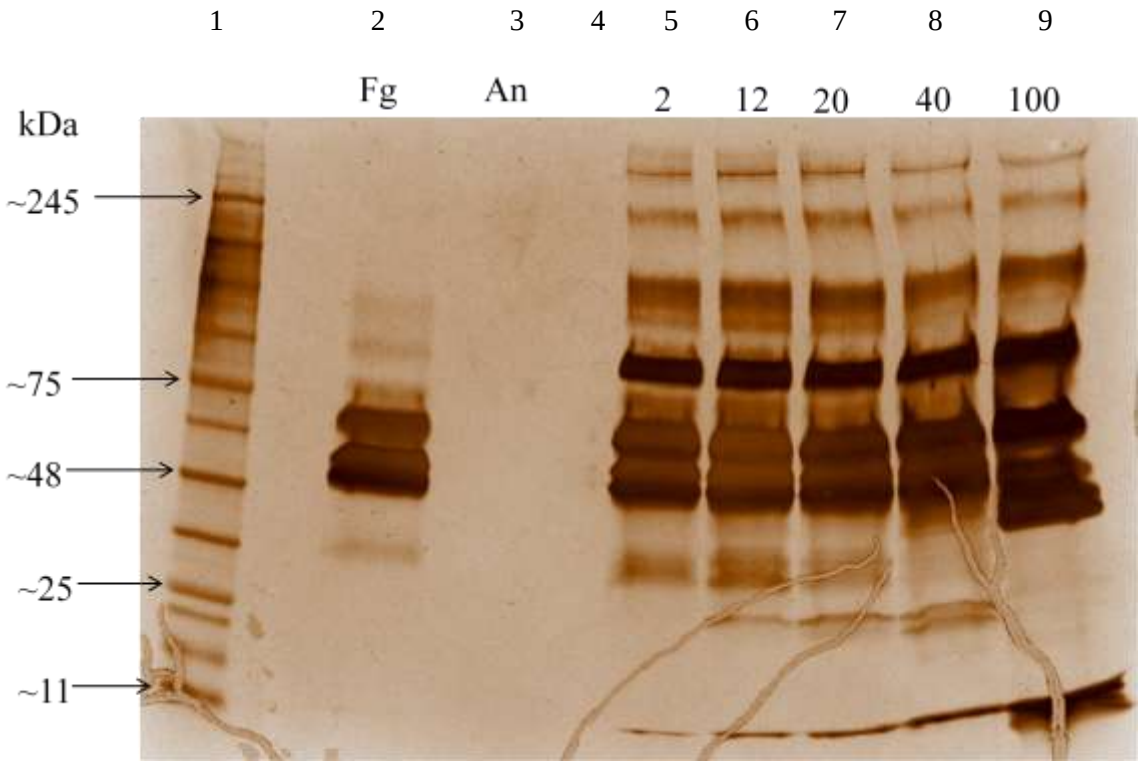

Figure 16. SDS-PAGE for detection of FDPs in Pn generation assays

Electrophoresis of enzymes was performed under reducing conditions in a discontinuous gradient gel (15% separating and 4% stacking gel). The proteins were stained with ProteoSilver ™ Silver Stain Kit. Lane 1 represents BLUeye pre- stained protein ladder. Lane 2 represents 3.3 µg of Fg; Lane 3 represents 0.6 U/ml of Ancrod, Lane 4 is blank, Lane 5 contains reaction mixture terminated at 2 min, Lane 6 contains reaction mixture terminated at 12 min, Lane 7 contains reaction mixture terminated at 20 min; Lane 8 contains reaction mixture terminated at 40 min; Lane 9 contains reaction mixture terminated at 100 min. Each reaction time course lane was loaded with 3.3 µg of Fg, 0.72 µg of Pg, 0.689 pg of tc- tPA and 0.6 U/ml of Ancrod

3.7 Comparison of k_2 values for inhibition of Pn±fibrin(ogen) by AT+UFH *versus* ATH

There were no significant differences between the k_2 values for inhibition of free Pn by ATH ($6.39 \times 10^6 \pm 0.59 \times 10^6 M^{-1}min^{-1}$) compared to the maximal inhibition achieved by AT+UFH ($5.74 \times 10^6 \pm 0.278 \times 10^6$) (figure 17). Furthermore, inclusion of either fibrin or fibrinogen resulted in a significant reduction in the k_2 values compared to free Pn for both AT+UFH and ATH (figure 17, table 1). However, this effect was less pronounced for ATH reactions. Therefore, protection from inhibition of approximately 75% is observed for AT+UFH, as opposed to 50% for ATH when fibrin(ogen) is present. Moreover, the k_2 values for inhibition of Pn±fibrin(ogen) by ATH were significantly ($p<0.05$) greater compared to those for AT+UFH, thus suggesting enhanced inhibition of fibrin(ogen)-bound Pn by the covalent conjugate.

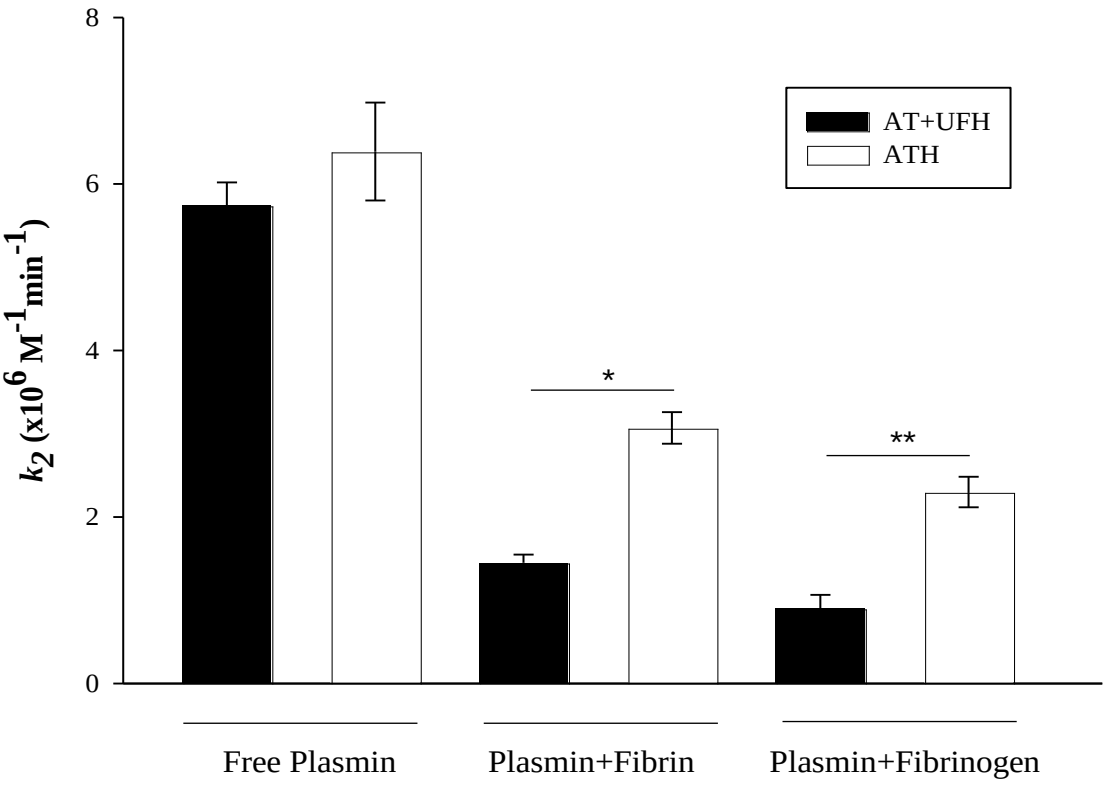

Figure 17. Inhibition of plasmin±fibrin(ogen) by AT+UFH versus ATH

Second-order rate constants (k_2 values) were measured under pseudo first-order conditions. Ten nM Pn was inhibited by either 100 nM AT and 3000 nM UFH or 100 nM ATH in the presence or absence of 100 nM of uncrosslinked fibrin or fibrinogen. The k_2 values are an average of n=5 ± standard error of mean. (*<0.01,**<0.05)

3.8 Detection of FPA from reaction of Fibrinogen with Ancrod

To confirm that Ancrod was cleaving FPA from the α chain of the fibrinogen molecule at the concentrations used in the rate experiments in section 3.6, a competitive ELISA was utilized. The FPA standard had an initial concentration of 55 ng/ml which was serially diluted to construct the standard curve. (Figure 18) A semi-log plot of absorbance values *versus* the concentrations of FPA was constructed and the equation for the line of best fit was utilized to deduce the concentration of FPA in the samples. The absorbance values obtained for the original Fg+Ancrod samples were not within the range of the standard curve. This was because the FPA concentration was too high for detection. Thus the sample was diluted to 1:80 to bring the absorbance within the standard curve. In comparison with the standard curve, and after correcting for dilution, the concentration of FPA in the original sample was determined to be 270.5 ng/ml (175 nM).This assay has allowed us to confirm that FPA is being released from fibrinogen by Ancrod thus allowing formation of fibrin.

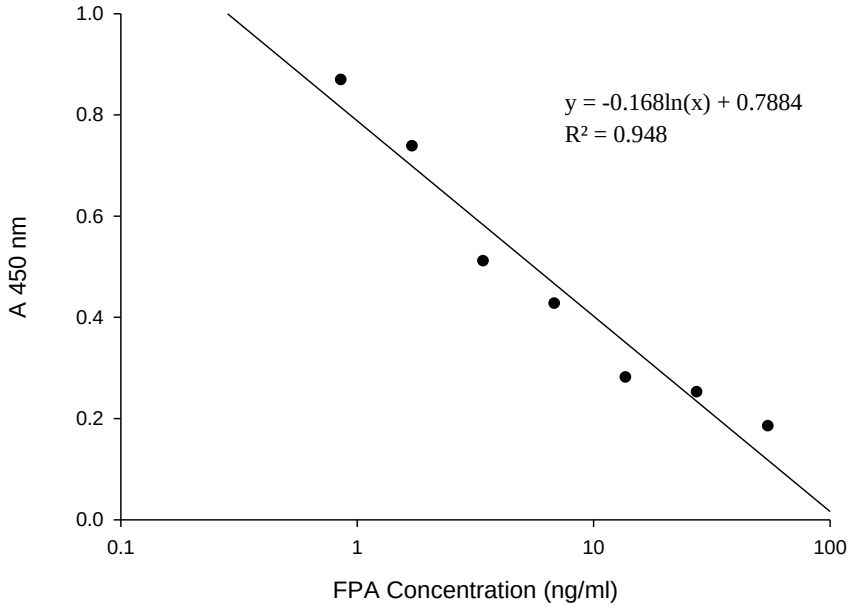

Figure 18. Standard curve for FPA samples

A Standard curve was constructed by serial dilution (1:1 – 1:64) of a 55ng/ml sample of purified FPA. FPA calibrator was incubated with affinity purified rabbit antibodies specific for FPA. The unreacted antibodies were then measured using a micro ELISA plate coated with synthetic FPA in which free antibodies bind to the immobilized FPA. Bound antibodies were detected by using a goat polyclonal antibody specific for rabbit IgG and coupled to HRP followed by development of color using TMB. There is an indirect relationship between the color developed and the concentration of FPA in the tested sample.

3.9 Studies of the mechanism for the protection of Pn

Potential mechanisms for Pn protection from ATH was investigated by utilizing excess UFH in the reactions, to see whether excess UFH may disrupt potential non-productive ternary complex formation between the UFH moiety of ATH, fibrin/fibrinogen and Pn. There was no statistically significant difference in the k_2 values for inhibition of Pn+fibrin or Pn+fibrinogen by ATH in the presence of excess UFH when compared to the values obtained in the absence of excess UFH (figure 19).

To assess whether the occupation of LBDs on the Pn molecule impacted the rate of inhibition by AT+UFH and ATH, Pn was incubated with EACA prior to inhibition. Rates achieved by AT+UFH and ATH for the inhibition of Pn+EACA were 1.7 and 1.4 fold lower, respectively, than those achieved for free Pn (figure 20). This may suggest that occupation of LBDs on Pn may in part play a role in the protective effect observed for both AT+UFH and ATH.

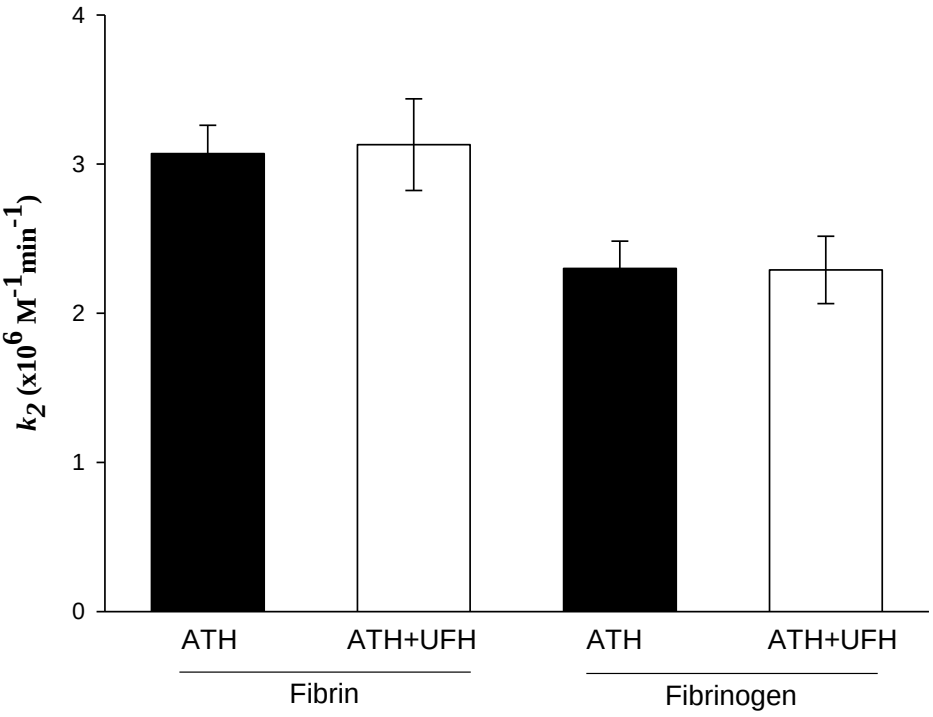

Figure 19. Inhibition of plasmin by ATH ±UFH

Excess (3000 nM) UFH was mixed with ATH and k_2 values for Pn inhibition were determined as previously described. The k_2 values are an average of n=5 ± standard error of mean

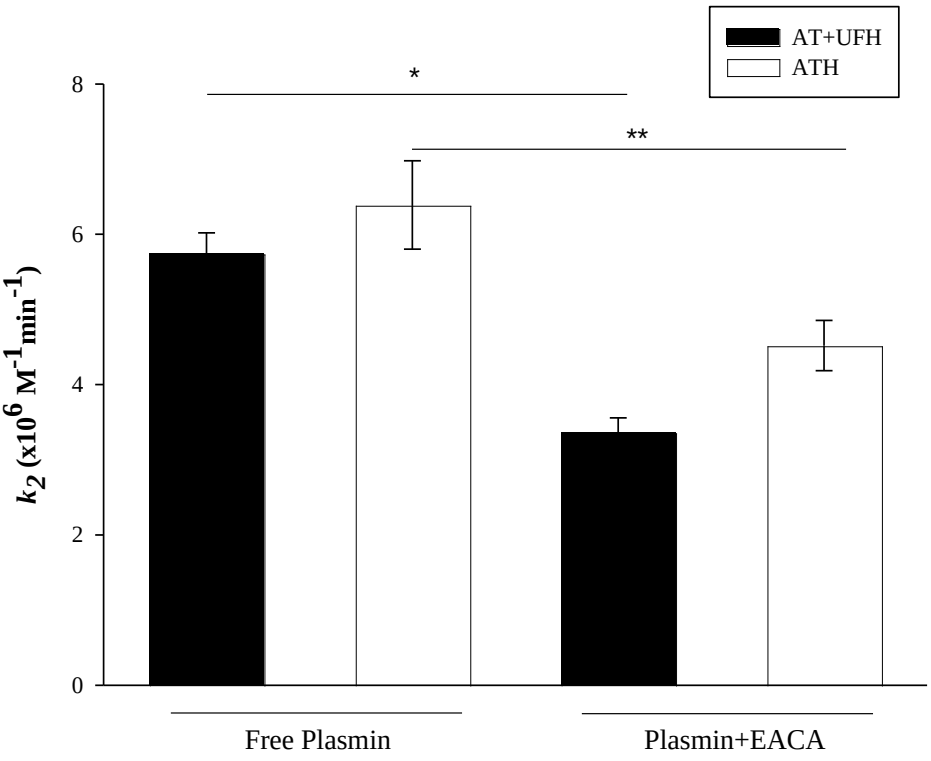

Figure 20. Effect of EACA on Pn inhibition by AT+UFH versus ATH.

EACA (200nM) was incubated with Pn and the k_2 values for inhibition by AT+UFH or ATH were determined as previously described. The k_2 values are an average of n=5 ± standard error of mean (*p<0.01,**p<0.05)

Table 1. k_2 values for the inhibition of plasmin under various conditions

CONDITION	AT+UFH(k_2 VALUES ± SD)	ATH (k_2 VALUES ± SD)
Free Pn	$5.74x10^6 \pm 0.278x10^6$	$6.39x10^6 \pm 0.588x10^6$
Pn + fibrin	$1.45x10^6 \pm 0.097x10^6$*	$3.07x10^6 \pm 0.192x10^6$
Pn + fibrinogen	$0.90x10^6 \pm 0.165x10^6$*	$2.30x10^6 \pm 0.183x10^6$
Pn + EACA	$3.36x10^6 \pm 0.197x10^6$	$4.52x10^6 \pm 0.334x10^6$

* $p<0.05$

3.10 Alterations in chromogenic activity of tPA

To further investigate the alterations in the rates of Pn generation seen in the above experiments we studied potential modulation of tPA by UFH, AT+UFH and ATH. This was studied by the incubation of increasing concentrations of the various reagents against a fixed concentration of tPA. For all reagents tested, no statistically significant difference in enzyme activity against a chromogenic substrate was observed at the concentrations of anticoagulants tested. (figure 21) This indicates that the reduction in rates of Pn generation seen above are very likely due to inhibition of the Pn (free or fibrin(ogen) bound) which is produced following tPA cleavage of Pg.

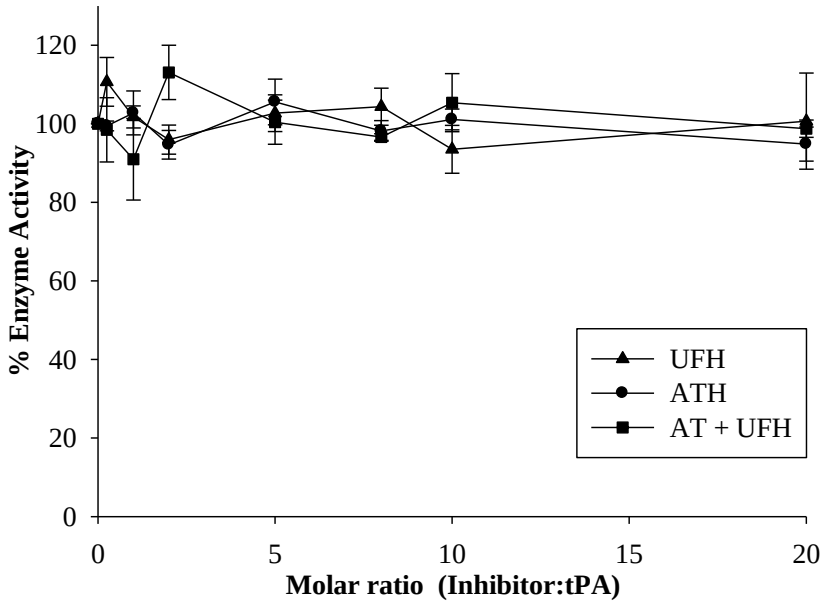

Figure 21. Comparison of tPA activity in the presence of UFH, AT+UFH and ATH Effects of anticoagulants on chromogenic activity were investigated. UFH, AT+UFH or ATH with a molar ratio range of 0 - 20 were titrated against a fixed concentration of tPA (20 nM) and allowed to incubate for a period of 15 min. Reactions were neutralized by simultaneous addition of a solution containing 1.25 mg/ml of polybrene and tPA substrate, S-2288 in buffer. Enzyme activity was then determined by measuring the rate of substrate cleavage (Vmax) for 10 min using a plate reader. No statistically significant differences were observed.

4. Discussion

Under physiological conditions, the coagulation and fibrinolytic pathways are slowly turning over and exist together in a fine balance. At the time of clot formation, fibrin deposition produces a stable crosslinked clot which is susceptible to proteolytic degradation through the actions of Pn generated from the fibrinolytic pathway. During thromboembolic states, local fibrin production exceeds the capacity of the fibrinolytic pathway, resulting in excessive clot formation. To limit clot development, anticoagulants such as UFH are administered under these circumstances. The interactions of UFH with the components of the coagulation cascade have been studied in great detail in the past and are well reported in the literature. However, the interactions of UFH with components of the fibrinolytic pathway have not been studied to the same extent and are not clearly understood. Some investigators have attempted to study the interactions of UFH with various fibrinolytic components. However, a discrepancy exists in the literature, which largely has been attributed to non-physiological experimental conditions. Previous investigations have shown that UFH(±AT) can increase Pn generation (9,95-100) whereas others have reported a reduction in Pn generation. (95) In addition, it has been reported that UFH can enhance the enzymatic activity of tPA, potentially augmenting Pn generation. (98) Furthermore, scarcely anything is known about potential ATH-fibrinolysis interactions. Many of the *in vitro* interactions of ATH with the various components of the coagulation cascade have been well characterized; however interactions of ATH with the fibrinolytic pathway have never been studied before. Therefore, in the present study, we have performed experiments which are

comparable to physiological conditions in an effort to understand the effects of AT+UFH and ATH on components of fibrinolysis.

4.1 Inhibition of Free Pn

We have observed that free Pn is susceptible to inhibition by AT and the rates of inhibition increase when catalyzed by UFH. It has previously been demonstrated that plotting k_2 *vs.* [UFH] can allow for the deduction of likely inhibition mechanisms for coagulation enzymes by AT+UFH. (3,14) In the current study the characteristic shape of the plot for Pn suggests that inhibition occurs through conformational AT activation and not through the template mediated mechanism, which is in agreement with previous reports. (3) In the conformational mechanism of inhibition, binding of AT to the high affinity pentasaccharide sequence of UFH, results in a conformational change in the AT molecule, which makes the RCL more susceptible to reaction with serine proteases. Additionally, we have observed that no significant difference exists between the rates of inhibition of free Pn for AT+UFH *versus* ATH. This comparison is consistent with our previous work showing that ATH displays rates of inhibition similar to AT+UFH for proteases inhibited via conformational activation of AT. (14) When comparing the rates for the inhibition of FIIa by AT+UFH (14) to the present results, it is apparent that k_2 values for inhibition of Pn are 2 to 3 orders of magnitude lower than for FIIa and that the rates of inhibition obtained in this study are comparable with previously reported rates. (3,4)

4.2 Inhibition of Pn Generation

Plasmin generation occurs by cleavage of plasminogen by a plasminogen activator. In this study we utilized a purified experimental system which contained all of the components necessary to generate Pn from Pg, including the cofactor fibrin. The rates of Pn generation observed in this study were comparable with previous reports utilizing similar conditions. (118) As expected, a decrease in the rates of Pn generation were observed upon the addition of either inhibitor (AT+UFH or ATH). ATH drastically reduced the rates of Pn generation compared to AT+UFH. The addition of ATH to the system resulted in essentially near zero rates of Pn generation, even at the lowest concentration tested. This may be explained by the efficient inhibition of both free and fibrin(ogen)-bound Pn by the covalent conjugate, thus preventing Pn from enhancing its own generation. As for AT+UFH, a significant reduction in the rates of plasmin generation were only seen when inhibitor concentrations were increased to 4-fold that of the original concentration. At the lowest concentration tested, AT+UFH resulted in a ~2.5 fold reduction whereas ATH resulted in a ~38 fold reduction. In this *in vitro* system utilized for calculating the generation of Pn, both forms of Pn, free and fibrin(ogen)-bound are presumably present and susceptible for neutralization by either inhibitor. Since plasmin can enhance its own generation by providing C-Lys residues on fibrin(ogen) (for both Pg and tPA), the inhibition of the plasmin formed from the activation of Pg by tPA, can in turn slow the rates of Pn generation under these conditions. Furthermore, it has been shown that FDPs can potentiate Pn generation much like fibrin (122), as seen in figure 13, there is a rapid increase in the absorbance values at 405 nm late in the assay

which may be explained by the generation of FDPs as is shown in the SDS-PAGE in figure 16.

4.3 Inhibition of Pn+fibrin(ogen)

To clarify the drastic differences observed in the reduction of the rates of Pn generation it was important to determine and compare rates of inhibition for free Pn and Pn in the presence of fibrin(ogen). This would clarify if Pn is being protected by fibrin(ogen) from inhibition. It is well known that surface-bound coagulation enzymes are protected from inhibition by AT+UFH, which has been implicated in clot propagation, even during anticoagulant therapy. (51) Moreover, we have previously shown that covalent linkage of AT to heparin allows for enhanced inhibition of these surface-bound coagulation factors. (106,114-116) In the present study we observed a reduction in the rates of inhibition for Pn+fibrin(ogen), indicating protection of the enzyme. In the presence of fibrin, a ~4-fold protective effect was observed in the presence of AT+UFH, whereas a milder ~2-fold protective effect was observed for ATH. In the presence of fibrinogen on the other hand, a more pronounced protection of Pn was observed for AT+UFH (6.4-fold), with a smaller change for ATH (2.8-fold). The rates of inhibition for Pn+fibrin(ogen) by ATH were significantly greater than AT+UFH under both conditions.

Although no significant differences were observed in the rates of inhibition of free Pn by AT+UFH or ATH, the more pronounced reduction in calculated rates of Pn generation when an intact fibrin clot was present by ATH might be explained by the inhibition of free Pn as well as an enhanced capability to inhibit fibrin-bound Pn. These findings are similar to those previously observed for inhibition of fibrin-bound FIIa or prothrombinase-complexed FXa (106,114-116). Mechanistically, these results can be

explained by the fact that, with AT+UFH non-covalent complex, UFH can dissociate from the AT to form ternary complexes with both fibrin and Pn. As such, two situations can occur: 1) the dissociation of UFH leaves the AT in the inactive state and unable to inhibit Pn, and 2) the UFH in the fibrin/UFH/Pn ternary complex creates a negative milieu around Pn, resulting in further repulsion of additional AT+UFH which prevents it from inhibiting the enzyme. As for ATH, the covalent linkage between heparin and AT prevents the dissociation of the heparin chain from the AT. Even if the heparin moiety of ATH forms non-productive complexes with fibrin or Pn, the covalent attachment of the AT molecule enables for proximal orientation of AT towards the enzyme with subsequent inhibition. This mechanism may, in part, explain the ~2-fold increase in the rate of inhibition observed for ATH compared to AT+UFH for Pn in the presence of fibrin. However, it still does not account for the ~2-fold reduction observed for Pn+fibrin relative to inhibition of free Pn by the ATH. It was possible that the relatively long heparin chains in ATH (average molecular weight of heparin chains in the conjugate is 18 kDa) (105) may also form non-productive complexes with fibrin and Pn to antagonize Pn inhibition. Approximately 33% of heparin chains in ATH have at least 2 very charged pentasaccharide sequences (124), thus the highly negative characteristic of the conjugated heparin molecules may also contribute to these interactions. Consequently, it was posited that addition of excess UFH with ATH may be able to displace any non-productive interactions of ATH with the fibrin and Pn. However, unlike previous work with prothrombinase, addition of excess UFH did not result in increased inhibition of Pn by the ATH. (115) This indicated that other mechanisms may be playing a role in protecting Pn from inhibition by AT+UFH or ATH.

Cumulatively, the data from the Pn generation experiments and inhibition of Pn±fibrin(ogen) suggests that ATH may be able to overcome the steric hindrance produced by fibrin(ogen) better than non-covalent AT in the presence of excess UFH. In addition, it has previously been shown that FDPs can protect Pn from inhibition by α_2AP (125), a similar mechanism may be playing a role in this study, although cross linked fibrin was not used in the assays reported here. In conclusion, these products, fibrin and UFH can bind Pn and lead to its steric hindrance, which potentially can be partly responsible for the reduced rates of inhibition observed in their presence. However, occupation of the LBDs may also be partly responsible for the reduction in rates observed in this study.

4.4 Mechanism of inhibition of Pn by AT+UFH and ATH

The serpin α_2AP is the major inhibitor of Pn *in vivo*.(45) It has been suggested that α_2AP inhibits Pn in a two-step mechanism in which first, the α_2AP interacts with LBDs on Pn followed by the reaction of the reactive centre loop with the active site of the protease. (48-50) Therefore, efficient inhibition of Pn by α_2AP is dependent on the availability of the LBDs on Pn. When Pn is bound to fibrin, LBDs on Pn are occupied thus potentially protecting Pn from reaction with inhibitors.

Schneider *et al* (53) utilized a system in which rates of inhibition of Pn by α_2AP were calculated in the presence of an intact FIIa-generated clot. Their data show that the rate of inhibition decreased from $9.5x10^6$ $M^{-1}min^{-1}$ to $3.2x10^6$ $M^{-1}min^{-1}$ immediately after clot formation. The rates of inhibition then continued to decrease (38-fold) as the fibrin clot was modified by Pn during with reaction progression. These findings suggest that both an intact fibrin clot and a Pn-modified fibrin clot can protect Pn from inhibition with

the modified form, imparting greater protection. This increase in protection can be explained by the exposure of C-Lys residues on the surface of the fibrin clot, allowing Pn to bind as the reaction progresses. Further, in the presence of TAFIa the protection observed with the Pn-modified fibrin is delayed while no change is observed in the presence of an intact fibrin clot. These findings suggest that the protection of Pn may be due to a combination of the steric hindrance produced by the intact fibrin clot in the initial stages of clot formation, and additionally due to binding of Pn to newly exposed C-Lys residues on the clot surface making the LBDs unavailable to the inhibitor. This aspect may also hold true for the current study in which we are studying inhibition of Pn by AT+UFH and ATH. Previous studies have also shown that in the presence of soluble fibrin surrogates, Pn can be protected 10-45 fold from inhibition by α_2AP. (48,49,125,126) Interestingly, Pn can also bind to initial products of fibrin degradation such as DD(E) where it can be protected from inhibition by α_2AP, with diminished protection being imparted by products subsequently produced by Pn proteolysis. (125)

To determine whether occupation of the LBDs on Pn may affect the abilities of AT+UFH or ATH to inhibit Pn, we utilized the synthetic Lys analog EACA which closely interacts with the LBDs on Pn. We observed that the rate of inhibition of Pn by both AT+UFH and ATH decreased proportionally in the presence of EACA. This may infer that LBDs located on the kringle domains on Pn may also be involved in the mechanisms of inhibition by AT. Perhaps the interactions of AT with Pn is dependent on the LBDs, and a two-step mechanism for inhibition of Pn by the AT is also important, similar to its homologous counterpart α_2AP. In the present study we observe a modest ~ 4- and ~2- fold reduction in inhibition of Pn by AT+UFH and ATH, respectively,

compared to the 10-45 fold reduction by α_2AP reported in literature. (48,49,125,126) However, additional investigations are required to confirm whether LBDs on Pn are directly interacting with AT and to what extent, the various forms of fibrin and FDPs protect Pn from inhibition by AT+UFH and ATH.

4.5 Summary and future directions

From the above results, we may potentially add to our understanding of the data we reported in previous *in vivo* studies showing a significant reduction in clot mass/size with the administration of ATH. Although a significant reduction in the calculated rates of Pn generation were observed *in vitro* in the current study, it can be speculated that the reduction in clot mass observed in the previously performed *in vivo* studies was mainly due to the superior ability of ATH to inhibit surface bound clotting factors such as cell surface bound FXa (as part of the prothrombinase complex) and fibrin bound FIIa in a fibrin clot, thus reducing clot propagation to a significant degree thus allowing the endogenous fibrinolytic pathway to degrade the clot. Since we observed that the k_2 values for inhibition of Pn±fibrin(ogen) by ATH were 2 to 3 orders of magnitude lower than those for FIIa (14), it can be suggested that the inhibitory activity of ATH towards FIIa is maintained while relatively sparing inhibition of Pn, so that Pn can continue degrading fibrin and restore hemostasis. Furthermore, in an *in vivo* system where other coagulation enzymes (FIIa, FXa) are present, at higher concentrations than Pn, ATH may react with those enzymes first, due to the greater rates of inhibition, and be less available for neutralizing Pn. In addition, although AT is able to inhibit Pn, it does so at a slower rate than α_2AP, maintaining α_2AP as the major regulator of Pn *in vivo*. (45) It is also likely that inhibitors of Pn other than α_2AP play a significant role only when the plasma

concentrations of Pn exceed the concentrations of α_2AP. However it can be speculated that with the administration of ATH, fibrin-bound Pn may be preferentially inhibited by ATH over α_2AP however rates of inhibition observed for either inhibitor are comparable (53). Taken altogether, it is more likely that ATH will preferentially inhibit coagulation factors over free or fibrin bound Pn allowing tipping of the balance in favor of clot dissolution. (figure 22)

In conclusion, this study provides some mechanistic understanding regarding the interactions of AT+UFH and the covalent ATH conjugate with components of the fibrinolytic system. Despite a significant effect on the *in vitro* rate of Pn generation in a purified system, ATH may not have strongly adverse affects on *in vivo* fibrinolysis, and may aid in the overall goal to reduce undesired thrombosis, primarily by inhibiting clot-bound thrombin. In addition, this study further supports the model that ATH has the ability to inhibit surface-bound enzymes more efficiently than AT+UFH. Although this investigation has the limitation that it only evaluated the fibrinolytic system in isolation, it provides a good understanding of the interactions between the purified inhibitors and some of the purified components of fibrinolysis. It is important to note that, unlike the studies of Schneider *et al.* we utilized fibrin forms which were pretreated with Pn and essentially are end point investigations. Further investigations are warranted which measure Pn inhibition by AT in real time in a dynamic system. Additional studied utilizing low molecular weight forms of Pn can also be utilized to determine these interactions which lack various K domains and would allow for the significance of binding of AT to the LBDs on Pn. It would also be of merit to utilize the model proposed by Schneider *et al.* to determine protection of Pn from inhibition by AT+UFH and ATH

as this will allow for the determination of the effects of different forms of fibrin on Pn protection, much like the original work which has demonstrated protection of Pn by α_2-AP. Lastly, to gain a better understanding of the effects of ATH on fibrinolysis, further studies should be performed in plasma-based systems and, ultimately, *in vivo*.

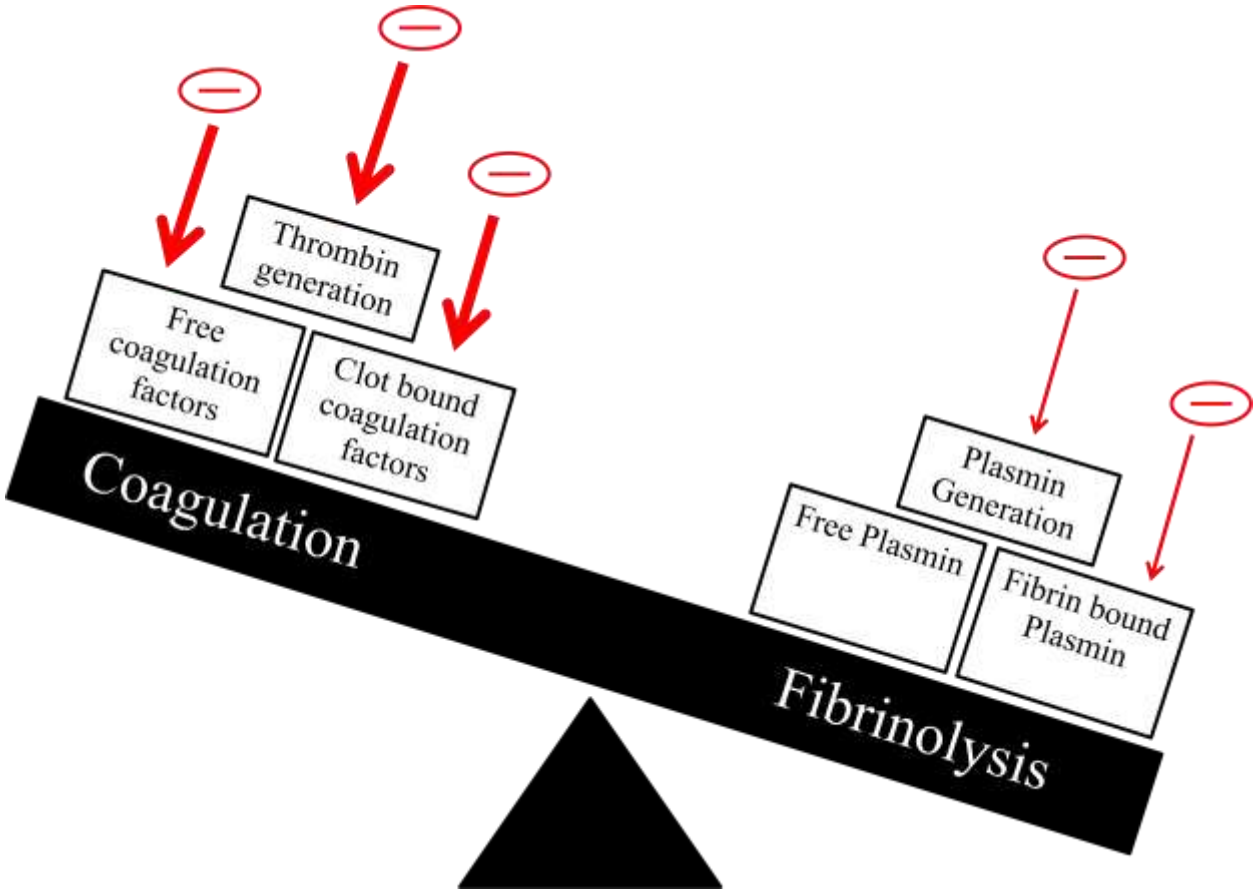

Figure 22. Graphical depiction of the effects of ATH *versus* AT+UFH in the balance between coagulation and fibrinolysis

ATH inhibits factors of the coagulation pathway 2-3 orders of magnitude faster than plasmin and may not adversely affect fibrinolysis, which may lead to enhanced clot degradation. Red arrows represent inhibition of respective components by the ATH compared to AT+UFH. Thickness of arrows represents degree of inhibition of the relative components depicted.

Reference List

(1) Nesheim ME. Thrombin and fibrinolysis. Chest 2003;124:33s-9s.

(2) Lee AY. Cancer and venous thromboembolism: prevention, treatment and survival. J Thromb Thrombolysis 2008;25:33-6.

(3) Jordan RE, Oosta GM, Gardner WT, Rosenberg RD. The kinetics of hemostatic enzyme-antithrombin interactions in the presence of low molecular weight heparin. J Biol Chem 1980;255:10081-90.

(4) Anonick PK, Wolf BB, Gonias SL. Regulation of plasmin, miniplasmin and streptokinase-plasmin complex by alpha 2 antiplasmin, alpha 2- macroglobulin, and antithrombin III in the presence of heparin. Thromb Res 1990;59:449-62.

(5) Semeraro N, Colucci M, Telesforo P, Collen D. The inhibition of plasmin by antithrombin-heparin complex I. in human plasma in vitro. Br J Haematol 1978;39:91-9.

(6) Collen D, Semeraro N, Telesforo P, Verstraete M. Inhibition of plasmin by antithrombin-heparin complex. II. during thrombolytic therapy in man. Br J Haematol 1978;39:101-10.

(7) Cofrancesco E, Vigo A, Pogliani EM. GAGs-potentiated inhibition of thrombin, factor Xa and plasmin in plasma and in a purified system containing antithrombin III-correlation with total charge density. Thromb Hemost 1981;46:749-51.

(8) Markwardt F, Klocking HP. Heparin-induced release of plasminogen activator. Hemostasis 1977;6:370-4.

(9) Paques EP, Stohr HA, Heimburger N. Study on the mechanism of action of heparin and related substances on the fibrinolytic system: Relationship between plasminogen activators and heparin. Thromb Res 1986;42:797-807.

(10) Vinazzer H, Stemberger A, Haas S, Blumel GB. Influences of heparin, of different heparin fractions and of a low molecular weight heparin-like substance on the mechanism of fibrinolysis. Thromb Res 1982;27:341-52.

(11) Kawamura H, Wantanbe I, Urano T, Takada Y, Takada A. The effects of polysaccharides on plasminogen activation by single chain-and two chain-tissue plasminogen activator. Thromb Res 1991;62:481-90.

(12) Andrade-Gordon P, Strickland S. Fractionation of heparin by chromatography on a tissue plasminogen activator-Sepharose column. Proc Natl Acad Sci USA 1990;87:1865-9.

(13) Simon DI, Fless GM, Scanu AM, Loscalzo J. Tissue type plasminogen activator binds to and is inhibited by surface-bound lipoprotein(a) and low density lipoprotein. Biochem 1991;30:6671-7.

(14) Patel S, Berry L, Chan AK. Analysis of inhibition rate enhancement by covalent linkage of antithrombin to heparin as a potential predictor of reaction mechanism. J Biochem 2006;141:25-35.

(15) Chan AK, Rak J, Berry L, Liao P, Vlasin M, Weitz J, et al. Antithrombin-heparin covalent complex:a possible alternative to heparin for arterial thrombosis prevention. Circulation 2002;106:261-5.

(16) Chan AK, Berry L, Klement P, Julian J, Mitchell L, Weitz J, et al. A novel antithrombin-heparin covalent complex: antithrombotic and bleeding studies in rabbits. Blood Coag Fibrinolysis 1998;9:587-95.

(17) Plow EF, Herren T, Redlitz A, Miles LA, Hoover-Plow JL. The cell biology of the plasminogen system. FASEB J 1995;9:939-45.

(18) Carmeliet P, Collen D. Development and disease in proteinase-deficient mice: Role of the plasminogen, matrix metalloproteinase and coagulation system. Thromb Res 1998;91:255-85.

(19) Adams GL, Manson RJ, Turner I, Sindram D, Lawson JH. The balance of thrombosis and hemorrhage in surgery. Hematol Oncol Clin North Am 2007;21:13-24.

(20) Mann K.G. Thrombin Formation. Chest 2003;124:4S-10S.

(21) Colman RW, Clowes AW, George JN. Overview of hemostasis. 5 ed. Lippincott Williams and Wilkins; 2006. p. 3-16.

(22) MacFarlane RG. An enzyme cascade in the blood clotting mechanism, and its function as a biochemical amplifier. Nature 1964;202:498-9.

(23) Davie EW, Ratnoff OD. Waterfall sequence for intrinsic blood clotting. Science 1964;145:1310-2.

(24) Smith SA. The cell based model of coagulation. J Vet Emerg Crit Care 2009;19:3-10.

(25) Butenas S, Mann KG. Kinetics of human factor VII activation. Biochem 1996;35:1904-10.

(26) Hoylaerts M, Rijken D, Lijnen HR, Collen D. Kinetics of the activation of plasminogen by human tissue plasminogen activator: role of fibrin. J Biol Chem 1982;257:2912-9.

(27) Menhart N, McCance SG, Sehl LC, Castellino FJ. Functional independence of the kringle 4 and kringle 5 regions of human plasminogen. Biochem 1993;32:8799-806.

(28) Lucas MA, Fretto LJ, McKee PA. The binding of human plasminogen to fibrin and fibrinogen. J Biol Chem 1983;258:4249-56.

(29) Saksela O. Plasminogen activation and regulation of pericellular proteolysis. Biochem Biophys Acta 1985;823:35-65.

(30) Holvoet P, Lijnen HR, Collen D. A monoclonal antibody specific for Lys-plasminogen: Application ot the study of the activation pathways of plasminogen in vivo. J Biol Chem 1985;260:12106-11.

(31) Pennica D, Holmes WE, Kohr WJ, Harkins RN, Vehar GA, Ward CA, et al. Cloning and expression of human tissue-type plasminogen activator cDNA in E.Coli. Nature 1983;301:214-21.

(32) Wallen P, Wiman B. Characterization of human plasminogen: II. Separation and partial characterization of different molecular forms of human plasminogen. Biochem Biophys Acta 1972;157:122-34.

(33) Fredenburgh JC, Nesheim ME. Lys-plasminogen is a significant intermediate in the activation of Glu-plasminogen during fibrinolysis in vitro. J Biol Chem 1992;267:26150-6.

(34) Markus G, Priore RL, Wissler FC. The binding of tranexamic acid to native (glu) and modified (lys) human plasminogen an its effects on conformation. J Biol Chem 1979;254:1211-6.

(35) de Vries C, Veerman H, Pannekoek H. Identification of the domains of tissue-type plasminogen activator involved in the augemted binding of fibrin after limited digestion with plasmin. J Biol Chem 1989;264:12604-10.

(36) Banyai L, Patthy L. Importance of intramolecular interactions in the control of the fibrin affinity and activation of human plasminogen. J Biol Chem 1984;259:6466-71.

(37) Suenson E, Lutzen O, Thorsen S. Initial plasmin-degredation of fibrin as the basis of a positive feed-back mechanism in fibrinolysis. Eur J Biochem 1984;140:513-22.

(38) Sottrup - Jensen L, Claeys H, Zajdel M, Petersen TE, Magnusson S. The primary structure of human plasminogen: isolation of two lysine - binding fragments and one mini plasminogen (MW, 38000) by elastase-catalyzed-specific limited proteolysis. Prog Chem Fibrinolysis Thrombolysis 1978;3:191-209.

(39) Gurewich V, Pannell R, Louie S, Kelly P, Suddith RL, Greenlee R. Effective and fibrin-specific clot lysis by a zymogen precursor from urokinase (pro-urokinase). A study in vitro and in two animal species. J Clin Invest 1984;73:1731-9.

(40) Linjen HR, Zamarron C, Blaber M, Winkler M, Collen D. Activation of plasminogen by pro-urokinase. J Biol Chem 1986;261:1253-8.

(41) Pizzo SV, Schwartz ML, Hill RL, McKee PA. The effect of plasmin on the subunit structure of human fibrin. J Biol Chem 1973;248:4574-83.

(42) Bajzar L, Manuel R, Neisheim ME. Purification and characterization of TAFI, a thrombin-activable fibrinolysis inhibitor. J Biol Chem 1995;270:14477-84.

(43) McKee PA. Tranexamic acid: a review of its use in the treatment of hyperfibrinolysis. Drugs 2012;72:585-617.

(44) Griffin JD, Ellman L. Epsilon-aminocaproic acid (EACA). Semin Thromb Hemost 1978;5:27-40.

(45) Collen D, Wiman B. Fast-acting plasmin inhibitor in human plasma. Blood 1978;51:563-9.

(46) Plow EF, Collen D. The presence and release of alpha-2-antiplasmin from human platelets. Blood 1981;58:1069-74.

(47) Travis J, Salvesan GS. Human plasma proteinase inhibitors. Ann Rev Biochem 1983;52:655-709.

(48) Wiman B, Collen D. On the kinetics of the reaction between human antiplasmin and plasmin. Eur J Biochem 1978;84:573-8.

(49) Wiman B, Bowman L, Collen D. On the kinetics of the reaction between human antiplasmin and low molecular weight form of plasmin. Eur J Biochem 1978;87:143-6.

(50) Wiman B, Collen D. On the mechanism of the reaction between human a_{2}-antiplasmin and plasmin. Eur J Biochem 1979;254:9291-7.

(51) Weitz JI, Hudoba D, Massel D, Maragonore J, Hirsh J. Clot-bound thrombin is protected from inhibition by heparin–antithrombin III but is susceptible to inactivation by antithrombin III-independent inhibitors. J Clin Invest 1990;86:385-91.

(52) Bruffato N, Ward A, Nesheim ME. Factor Xa is highly protected from antithrombin-fondaparinux and antithrombin-enoxaparin when incorporated in the prothrombinase complex. J Thromb Hemost 2003;1:1258-63.

(53) Schneider M, Nesheim ME. A study of the protection of plasmin from antiplasmin inhibition within an intact fibrin clot during the course of clot lysis. J Biol Chem 2004;279:13333-9.

(54) Anonick PK, Gonias SL. Soluble fibrin preparations inhibit the reaction of plasmin with alpha 2-macroglobulin. Comparison with alpha 2-antiplasmin and leupeptin. Biochem J 1991;275:53-59.

(55) Cesaurman-Maus G, Hajjar KA. Molecular mechanisms of fibrinolysis. Br J Haematol 2005;129:307-21.

(56) Aoki N, Maroi M, Tachiya K. Effects of alpha-2-plasmin inhibitor on fibrin clot lysis. Its comparison with alpha-2-macroglobulin. Thromb Hemost 1978;39:22-31.

(57) Ny T, Sawdey M, Lawrence D, Millan JL, Loskutoff DJ. Cloning and sequence of a cDNA coding for the human beta-migrating endothelial-cell-type plasminogen activator inhibitor. Proc Natl Acad Sci USA 1986;83:6776-80.

(58) Samad F, Yamamoto K, Loskutoff DJ. Distribution and regulation of plasminogen activator inhibitor-1 in murine adipose tissue in vivo. J Clin Invest 1996;97:37-46.

(59) Hijjar KA. The molecular basis of fibrinolysis. Hematology of Infancy and Childhood.Philadelphia: W.B Saunders Co.; 2003. p. 1497-514.

(60) Ye RD, Aherns SM, Le Beau MM, Lebo RV, Sadler JE. Structure of the gene for human plasminogen activator inhibitor-2. The nearest mammalian homologue of chicken ovalbumin. J Biol Chem 1989;264:5495-502.

(61) O'Gara PT, Kushner FG, Ascheim DD, et al. ACCF/AHA guideline for the management of ST-elevation myocardial infarction: A report of the American College of Cardiology Foundation/American Heart Association Task Force on Practice Guidelines. J Am Coll Cardiol 2013;61:e78-e140.

(62) Castellino FJ, Ploplis VA. Structure and function of plasminogen/plasmin system. Thromb Hemost 2005;93:647-54.

(63) Irving J.A, Pike P.N, Lesk A.M, Whisstock J.C. Phylogeny of the serpin superfamily: Implications of patterns of amino acid conservation for structure and function. Genome Research 2000;10:1845-64.

(64) Quinsey N.S, Greedy A.L, Bottomley S.P, Whisstock J.C, Pike P.N. Antithrombin: in control of coagulation. Int J Biochem Cell Biol 2004;36:386-9.

(65) Damus P, Hicks M, Rosenberg RD. Anticoagulant action of heparin. Nature 1973;246:355-7.

(66) Olds RJ, Lane DA, Chowdhury V, Thein SL. Antithrombin:the prinicipal inhibitor of thrombin. Semin Thromb Hemost 1994;20:353-72.

(67) Rao LV, Nordfang O, Hoang AD, Pendurthi UR. Mechanism of antithrombin III inhibition of factor VIIa/tissue factor activity on cell surfaces. Comparison with tissue factor pathway inhibitor/factor Xa-induced inhibition of factor VIIa/tissue factor activity. Blood 1995;85:121-9.

(68) Rosenberg JS, McKenna PW, Rosenberg RD. Inhibition of human factor IXa by human antithrombin. J Biol Chem 1975;250:8883-8.

(69) Stead N, Kaplan AP, Rosenberg RD. Inhibition of activated factor XII by antithrombin-heparin cofactor. J Biol Chem 1976;251:6481-8.

(70) Chandra T, Stackhouse R., Kidd VJ, Robson K, Woo SLC. Sequence homology between human alpha 1-antichymotrypsin, alpha 1-antitrypsin and antithrombin III. Biochemistry 1983;22:5055-61.

(71) Lawrence DA, Ginsburg D, Day DE, Berkenpas MB, Verhamme IM, Kvassman JO, et al. Serpin-protease complexes are trapped at stable acyl-enzyme intermediates. J Biol Chem 1995;270:25309-12.

(72) Desai UR, Petitou M., Bjork I, Olson ST. Mechanism of heparin activation of antithrombin: evidence for an induced-fit model of allosteric activation involving two interaction subsites. Biochemistry 1998;37:13033-41.

(73) Stavridi ES, O'Malley K, Lukacs CM, Moore WT, Lambaris JD, Christianson DW, et al. Structural changes in alpha-chymotrypsin induced by completion with alpha 1-antichymotrypsin as seen by enhanced sensitivity to proteolysis. Biochemistry 1996;35:10608-15.

(74) Picard V, Ersdal-Badju E, Bock SC. Partial glycosylation of antithrombin III asparagine-135 is caused by the serine in the third position of its N-glycosylation consensus sequence and is responsible for production of the beta-antithrombin III isoform with enhanced heparin affinity. Biochemistry 1995;34:8433-40.

(75) Linhardt RJ, Ampofo SA, Fareed J. Isolation and characterization of human heparin. Biochemistry 1992;31:12441-5.

(76) Stringer SE, Kandola BS, Pye DA. Heparin sequencing. Glycobiology 2003;13:97-107.

(77) Avraham S, Stevens RL, Nicodemus CF, Gartner MC Susten KF, Weis JH. Molecular cloning of a cDNA that encodes the peptide core of a mouse mast cell secretory granule proteoglycan and comparison with the analogous rat and human cDNA. Proc Natl Acad Sci USA 1989;263:3763-7.

(78) Avraham S, Stevens RL, Gartner MC, Austen KF, Lalley PA, Weis JH. Isolation of a cDNA that encodes the peptide core of the secretory granule proteoglycan of

rat basophilic leukemia-1 cells and assessment of its homology to the human analogue. J Biol Chem 1988;263:7292-6.

(79) Gallagher JT, Walker A. Molecular distinctions between heparan sulphate and heparin. Analysis of sulphation patterns indicates that heparan sulphate and heparin are separate families of N-sulphated polysaccharides. Biochem J 1985;230:665-74.

(80) Rosenberg RD, Damus PS. The purification and mechanism of action of human antithrombin-heparin cofactor. J Biol Chem 1973;248:6490-505.

(81) Rosenberg RD. Redesigning Heparin. N Engl J Med 2001;344:673-5.

(82) Huntington JA, Olson ST, Fan B., Gettings AL. Mechanism of heparin activation of antithrombin. Evidence for a reactive center loop preinsertion with expulsion upon heprin binding. Biochemistry 1996;35:8495-503.

(83) Jin L., Abrahams J.P, Skinner R, Petitou M, Pike P.N. The anticoagulant activation of antithrombin by heparin. Proc Natl Acad Sci USA 1997;94:14683-8.

(84) Olson ST, Bjork I, Sheffer R, Craig PA, Shore JD, Choay J. Role of the antithrombin-binding pentasaccharide in heparin acceleration of antithrombin-proteinase reactions. Resolution of the antithrombin conformational change contribution to heparin rate enhancement. J Biol Chem 1992;267:12528-38.

(85) Danielsson AE, Raub E, Lindahl U, Bjork I. Role of ternary complexes in which heparin binds both antithrombin and proteinase, in the acceleration of the reaction between antithrombin and thrombin or factor Xa. J Biol Chem 1986;261:15467-73.

(86) Li W, Johnson DJ, Esmon CT, Huntington JA. Structure of the antithrombin-thombin-heparin teranary complex reveals the antithrombotic mechanism of heparin. Nat Struct Mol Biol 2004;11:857-62.

(87) Young E, Prins M., Levine J., Hirsh J. Heparin binding to plasma proteins, an important mechanism for heparin resistance. Thromb Haemost 1992;67:639-43.

(88) Jaques LB, Mahadoo J., Kavanagh LW. Intrapulmonary heparin. A new procedure for anticoagulation therapy. Lancet 1976;2:1157-61.

(89) Hirsh J, van Aken WG, Gallus AS., Dollery CT., Cade JF., Yung WL. Heparin kinetics in venous thrombosis and pulmonary embolism. Circulation 1976;53:691-5.

(90) Bruffato N, Ward A, Nesheim ME. Factor Xa is highly protected from antithrombin-fondaparinux and antithrombin-enoxaparin when incorporated into the prothrombinase complex. J Thromb Haemost 2010;1:1258-63.

(91) Hogg PJ, Jackson CM. Fibrin monomer protects thrombin from inactivation by heparin–antithrombin III: implications for heparin efficacy. Proc Natl Acad Sci USA 1989;86:3619-23.

(92) Eisenberg PR. Role of heparin in coronary thrombolysis. Chest 1992;101:131S-9S.

(93) Hatton MWC, Berry LR, Machovich R, Regoeczi E. Titration of commercial heparins by reaction with NaB^3H^4: chemical analysis and biological properties of the product. Anal Biochem 1980;106:417-26.

(94) Olson ST, Bjork I, Shore JD. Kinetic characterization of heparin-catalyzed and uncatalyzed inhibition of blood coagulation proteinases by antithrombin. Methods Enzymol 1993;222:525-59.

(95) Young TN, Edelberg JM, Stack S, Ploug M. Ionic modulation of the effects of heparin on plasminogen activation by tissue plasminogen activator: the effects of ionic strength, divalent cations, and chloride. Arch Biochem Biophys 1992;296:530-8.

(96) Edelberg JM. Kinetic analysis of the effects of heparin and lipoproteins in tissue plasminogen activator mediated plasminogen activation. Biochemistry 1990;29:5906-11.

(97) Soeda S, Kakiki M, Shimeno H, Nagamatsu A. Localization of the binding sites of porcine tissue type plasminogen activator and plasminogen activation. Biochem Biophys Acta 1987;916:279-87.

(98) Liang JF, Li Y, Yang VC. The potential mechanism for the effect of heparin on tissue plasminogen activator–mediated plasminogen activation. Thrombosis Research 2000;97:349-58.

(99) Rijken D, de Munk GA, Jie AF. Interaction of plasminogen activators and plasminogen with heparin:effect of ionic strength. Thromb Hemost 1993;70:867-72.

(100) Andrade-Gordon P, Stickland S. Interaction of heparin with plasminogen activators and plasminogen: effects on the activation of plasminogen. Biochemistry 1986;25:4033-40.

(101) Weitz J.I, Kuint J, Leslie B, Hirsh J. Standard and low molecular weight heparin have no effect on tissue plasminogen activator induced plasma clot lysis or fibrinogenolysis. Thromb Hemost 1991;65:541-4.

(102) Ceustermans R, Hoylaerts M, De Mol M, Collen D. Preperation,characterization, and turnover properties of heparin-antithrombin III complexes stabalized by covalent bonds. J Biol Chem 1982;257:3401-8.

(103) Bjork I, Larm O, Lindahl U, Nordling K, Riquelme ME. Permanent activation of antithrombin by covalent attachment of heparin olgosaccharides. FEBS Lett 1982;143:96-100.

(104) Mitra G, Jordan RE, inventors; Covalently bound heparin-antithrombin III complex. Miles Laboratories Inc. United States patent 536072. 1983.

(105) Chan A, Berry L, O'Brodovich H, Klement P, Mitchell L, Baranowski B, et al. Covalent antithrombin-heparin complexes with high anticoagulant activity. Intravenous, subcutaneous, and intratracheal administration. J Biol Chem 1997;272:22111-7.

(106) Berry L, Becker D.L, Chan AK. Inhibition of fibrin-bound thrombin by a covalent antithrombin-heparin complex. J Biochem 2002;132:167-76.

(107) Berry L, Stafford A, Fredenburgh A, O'Brodovich H, Mitchell L, Weitz J, et al. Investigation of the anticoagulation mechanisms of a covalent antithrombin-heparin complex. J Biol Chem 1998;273:34730-6.

(108) Valassara H, Brownlee M, Cerami A. Advanced non-enzymatic tissue glycosylation: significance in late diabetic complications. Diabetes Res Clin Pract 1989;7:S103-S109.

(109) Sakurai T, Boissel JP, Bunn HF. Non-enzymatic glycation of antithrombin III in vitro. Biochem Biophys Acta 1988;946:340-7.

(110) Mewhort-Buist TA, Junop M, Berry LR, Chindemi P, Chan AK. Structural effects of a covalent linkage between antithrombin and heparin: Covalent N-terminal attachement of heparin enhances the maintenance of antithrombin's actovated state. J Biochem 2006;140:175-84.

(111) Berry L, Chan A, Andrew M. Polypeptide-polysaccharide conjugates produced by spontaneous non-enzymatic glycation. J Biochem 1998;124:434-9.

(112) Chan AK, Berry LR, Paredes N, Parmar N. Isoform composition of antithrombin in a covalent antithrombin-heparin complex. Biochem Biophys Res Commun 2003;309:986-91.

(113) Frebelius S, Isaksson S, Swedenborg J. Thrombin inhibition by antithrombin III on the subendothelium is explained by the isoform AT beta. Arterioscler Thromb Vasc Biol 1996;16:1292-7.

(114) Stevic I, Chan HH, Chander A, Berry LR, Chan AK. Covalently linking heparin to antithrombin enhances prothrombinase inhibition on activated platelets. Thromb Hemost 2013;109:[Epub ahead of print].

(115) Stevic I, Berry LR, Chan AKC. Mechanism of inhibition of the prothrombinase complex by a covalent antithrombin-heparin complex. J Biochem 2012;152:139-48.

(116) Stevic I, Chan AKC, Berry LR, Chander A, Chan AK. Inhibition of the prothrombinase complex on red blood cells by heparin and covalent antithrombin-heparin complex. J Biochem 2013;153:103-10.

(117) Chan AK, Pardes N, Thong B, Chindemi P, Paes B, Berry LR, et al. Binding of heparin to plasma proteins and endothelial surfaces is inhibited by covalent linkage to antithrombin. Thromb Hemost 2004;91:1009-18.

(118) Kim PY, Tieu LD, Stafford AR, Fredenburgh JC, Weitz J. A high affinity interaction of plasminogen with fibrin is not essential for efficient activation by tissue type plasminogen activator. J Biol Chem 2012;287:4652-61.

(119) Ewart MR, Hatton MWC, Basford JM, Dodgson KS. The proteolytic action of Arvin on human fibrinogen. Biochem J 1970;118:603-9.

(120) Senis YA, Kim PY, Fuller GL, Garcia A, Prabhakar S, Watson SP, et al. Isolation and characterization of cotiaractivase a novel low weight prothrombin activator from the venom of *Bothrops cotiara*. Biochem Biophys Acta 2006;1764:863-871.

(121) Hatton MWC. Studies on the coagulant enzyme from Agkistrodon Rhodostoma venom. Isolation and some properties of the enzyme. Biochem J 1973;131:799-807.

(122) Weitz J.I, Leslie B, Ginsberg J. Soluble fibrin degradation products potentiate tissue plasminogen activator induced fibrinogen proteolysis. J Clin Invest 1991;87:1082-90.

(123) Mosesson MW, Siebenlist KR, Hernandez I, Lee KN, Christiansen VJ, McKee PA. Evidence that alpha2-antiplasmin becomes covalently ligated to plasma fibrinogen in the circulation: a new role for plasma factor XIII in fibrinolysis regulation. J Thromb Haemost 2008;6:1565-70.

(124) Hogg PJ, Jackson CM., Labanowski JK, Bock PE. Binding of fibrin monomer and heparin to thrombin in a ternary complex alters the environment of the thrombin catalytic site, reduces affinity for hirudin, and inhibits cleavage of fibrinogen. J Biol Chem 1996;271:26088-95.

(125) Lee AY, Fredenburgh JC, Stewart RJ, Rischke JA, Weitz J. Like fibrin, (DD)E, the major degradation product of crosslinked fibrin, protects plasmin from inhibition by alpha 2-antiplasmin. Thromb Hemost 2001;85:502-8.

(126) Anonick PK, Gonias SL. Kinetics of the reaction of streptokinase-plasmin complex with purified human and mouse alpha 2-macroglobulin. Implications for mechanism. Biochem J 1989;264:745-52.